UC Santa Cruz

Title

Measurement of the centrality and pseudorapidity dependence of the integrated elliptic flow in lead—lead collisions at sNN=2.76 TeV with the ATLAS detector

Permalink

https://escholarship.org/uc/item/7n71n64r

Journal

ISSN

Authors

The ATLAS Collaboration
Aad, G
Abbott, B
et al.

Publication Date

DOI

Copyright Information

Peer reviewed

THE EUROPEAN
PHYSICAL JOURNAL C

Measurement of the centrality and pseudorapidity dependence of the integrated elliptic flow in lead–lead collisions at $\sqrt{s_{NN}} = 2.76$ TeV with the ATLAS detector

The ATLAS Collaboration[⋆]

CERN, 1211 Geneva 23, Switzerland

Abstract The integrated elliptic flow of charged particles produced in Pb+Pb collisions at $\sqrt{s_{NN}} = 2.76$ TeV has been measured with the ATLAS detector using data collected at the Large Hadron Collider. The anisotropy parameter, v_2, was measured in the pseudorapidity range $|\eta| \leq 2.5$ with the event-plane method. In order to include tracks with very low transverse momentum p_T, thus reducing the uncertainty in v_2 integrated over p_T, a 1 μb^{-1} data sample recorded without a magnetic field in the tracking detectors is used. The centrality dependence of the integrated v_2 is compared to other measurements obtained with higher p_T thresholds. The integrated elliptic flow is weakly decreasing with $|\eta|$. The integrated v_2 transformed to the rest frame of one of the colliding nuclei is compared to the lower-energy RHIC data.

1 Introduction

The anisotropy in the azimuthal angle distribution of particles produced in heavy-ion collisions has been studied extensively due to its sensitivity to the properties of the produced hadronic medium [1,2]. The final-state anisotropy arises from the initial spatial asymmetry of the overlap zone in the collision of two nuclei with non-zero impact parameter. The initial spatial asymmetry induces asymmetric pressure gradients that are stronger in the direction of the reaction plane and, due to the collective expansion, lead to an azimuthally asymmetric distribution of the ejected particles. The final-state anisotropy is customarily characterized by the coefficients v_n of the Fourier decomposition of the azimuthal angle distribution of the emitted particles [3]. The second Fourier coefficient v_2 is related to the elliptical shape of the overlap region in non-central heavy-ion collisions, and the higher flow harmonics reflect fluctuations in the initial collision geometry [4]. The first observation of elliptic flow, quantified by measurements of v_2, at RHIC [5–8] were found to be well

described by predictions based on relativistic hydrodynamics [9–11], providing compelling evidence that the created matter is strongly coupled and behaves like an almost perfect, non-viscous, fluid. Later studies show small deviations from ideal hydrodynamics, described in terms of the ratio of shear viscosity to entropy density [12–15].

First results from Pb+Pb collisions at $\sqrt{s_{NN}} = 2.76$ TeV [16–21] from the Large Hadron Collider (LHC) showed no change in the transverse momentum, p_T, dependence of elliptic flow from that measured at the highest RHIC energy, while the elliptic flow integrated over p_T [16,20] was found to increase by about 30 % from the RHIC energy of $\sqrt{s_{NN}} = 200$ GeV[1] to $\sqrt{s_{NN}} = 2.76$ TeV at the LHC. This increase in the integrated elliptic flow with energy is therefore driven mostly by the increase in the mean p_T of the produced particles. The dependence of elliptic flow on the geometry of the collision (the collision centrality) is of particular importance, since the flow is thought to depend strongly on the initial spatial anisotropy. Hydrodynamical models are used to quantitatively relate the initial geometry to the experimentally measured distributions. Furthermore, recent hydrodynamical calculations [22,23] also include a longitudinal dependence in the source shape, which can be deduced from flow measurements over a wide pseudorapidity range.

This article presents measurements of the centrality and pseudorapidity dependence of the elliptic flow integrated over the p_T of charged particles produced in Pb+Pb collisions at $\sqrt{s_{NN}} = 2.76$ TeV recorded in 2010 by the ATLAS detector.

In order to reduce the uncertainty in the p_T-integrated coefficient v_2 by including tracks with p_T lower than in the measurements reported by the ALICE [16] and CMS [20] experiments, a special track reconstruction procedure was applied to "field-off" data taken without the solenoid's magnetic field in the tracking detectors. Other track recon-

---

[1] ATLAS uses the system of units where $c = \hbar = 1$.

struction methods, applicable at higher p_T, were exploited in cross-checks using "field-on" data taken with the solenoid's magnetic field.

2 The ATLAS detector

The ATLAS detector is a multi-purpose particle physics apparatus and is described in detail elsewhere [24]. This analysis uses the three-level trigger system to select Pb+Pb collision events, the forward calorimeters (FCal) to measure the collision centrality, and the inner detector (ID) to measure charged-particle tracks. The ID tracking system comprises silicon pixel and microstrip detectors and a transition radiation tracker. It provides complete azimuthal coverage and spans the pseudorapidity region $|\eta| < 2.5$.[2] The pixel detector consists of a three-layer barrel section and three discs in each of the forward regions. The semiconductor tracker has four double layers of microstrip sensors in its barrel section and nine discs in each of the forward regions. The ID is surrounded by a thin superconducting solenoid, which produces a 2 T axial magnetic field for the field-on data. The FCal measures both electromagnetic and hadronic energy, using copper–tungsten/liquid-argon technology, and provides complete azimuthal coverage for $3.2 < |\eta| < 4.9$. The hardware-based Level-1 trigger selected minimum-bias Pb+Pb collisions by requiring either a coincidence of signals recorded in the zero-degree calorimeters (ZDC) located symmetrically at $z = \pm 140$ m ($|\eta| > 8.3$) or a signal in at least one side of the minimum-bias trigger scintillators (MBTS) at $z = \pm 3.6$ m ($2.1 < |\eta| < 3.9$). To suppress beam backgrounds, the Level-2 trigger demanded MBTS signals from opposite sides of the interaction region and imposed a timing requirement on them.

With these trigger conditions, ATLAS recorded a sample of Pb+Pb collisions corresponding to an integrated luminosity of approximately 1 μb^{-1} taken with the field provided by the solenoid turned off. In addition, approximately 0.5 μb^{-1} of field-on data was used in studies of track reconstruction performance.

3 Event selection and centrality definition

The offline event selection required each event to have a vertex formed by at least three charged-particle tracks recon-

structed in the ID. The data were recorded at low instantaneous luminosity where the probability of multiple collisions per bunch crossing (pile-up) was negligible. The track reconstruction algorithms therefore allowed only one collision vertex (called the primary vertex) in each event, thereby reducing the processing time while maintaining efficiency. The time difference between the MBTS signals from the opposite sides of the interaction region was required to be less than 3 ns, and a coincidence of ZDC signals was also required. These additional selection criteria efficiently remove beamgas and photo-nuclear interactions. As shown in previous studies [18], the applied trigger and offline requirements provide a minimum-bias event sample in which the fraction of inelastic Pb+Pb collisions is 98 ± 2 %.

Events satisfying the above criteria were also required to have a primary vertex within 50 mm (100 mm) in the z-direction of the nominal centre of the ATLAS detector for the field-off (field-on) data subsample. After requiring all relevant subdetectors to be performing normally, the subsamples used in the analysis of the field-off and field-on data contained approximately 1.6 million and 3 million minimumbias events, respectively.

Monte Carlo (MC) event samples were used to determine the tracking efficiencies and the rates of fake tracks. The HIJING event generator [25] was used to produce minimumbias Pb+Pb collisions. Events were generated with the default parameters except for jet quenching, which was turned off. The effect of elliptic flow was implemented after event generation. The azimuthal angles of final-state particles were redistributed at generator level to produce an elliptic flow consistent with previous ATLAS measurements [18,19]. The simulation of the ATLAS detector's response [26] to the generated events is based on the GEANT4 package [27] and included a detailed description of the detector geometry and material in the 2010 Pb+Pb run. Two samples of 0.5 million MC events were simulated, one with the solenoid field switched off and the other with it switched on. Additional MC samples consisting of 50,000 events simulated with 10–20 % extra detector material were used to study systematic uncertainties. The generated charged particles were reweighted with p_T- and centrality-dependent functions so that the p_T spectra in the MC samples matched the experimental ones [28].

The centrality of the Pb+Pb collisions was characterized by the summed transverse energy, ΣE_T^{FCal}, measured in the FCal [18]. The ΣE_T^{FCal} distribution was divided into ten centrality bins, each representing 10 % of the full distribution after accounting for 2 % inefficiency in recording the most peripheral collisions (the 0–10 % centrality interval corresponds to the most central 10 % of collisions: those with the largest ΣE_T^{FCal}). A small change in the overall recording efficiency leads to large fluctuations in the population of the most peripheral collisions. To avoid resulting large sys-

---

[2] ATLAS uses a right-handed coordinate system with its origin at the nominal interaction point (IP) in the centre of the detector and the z-axis along the beam pipe. The x-axis points from the IP to the centre of the LHC ring, and the y-axis points upward. Cylindrical coordinates (r, ϕ) are used in the transverse plane, ϕ being the azimuthal angle around the beam pipe. The pseudorapidity is defined in terms of the polar angle θ as $\eta = -\ln\tan(\theta/2)$.

tematic uncertainties, the 20 % of events with the smallest ΣE_T^{FCal} were not included in the analysis.

4 Elliptic-flow measurement

The final-state azimuthal anisotropy is quantified by the coefficients in the Fourier expansion of the ϕ distribution of charged particles [3],

$$dN/d\phi \propto 1 + 2\sum_{n=1}^{\infty} v_n \cos\left(n[\phi - \Psi_n]\right), \tag{1}$$

where v_n and Ψ_n are the magnitude and the azimuthal direction (called the event-plane angle) of the n-th flow harmonic, respectively.

The second flow harmonic, v_2, for a given collision centrality is a function of p_T and η, and is determined by

$$v_2(\eta, p_T) = \frac{\langle \cos(2[\phi - \Psi_2])\rangle}{\sqrt{\langle \cos(2[\Psi_2^N - \Psi_2^P])\rangle}}, \tag{2}$$

where the numerator denotes the average over charged-particle tracks in a given η and p_T range, and the denominator, averaged over events, is a correction accounting for the finite experimental resolution in the determination of the event-plane angle Ψ_2. This resolution correction was obtained using the sub-event technique [3] as described in Refs. [18,19]. The two "sub-events" defined for each event cover two η ranges of the same width in the positive and negative η hemispheres ($3.2 < |\eta| < 4.8$) of the FCal detector. The sub-event-plane angles are determined by

$$\Psi_2^{N(P)} = \frac{1}{2}\tan^{-1}\left(\frac{\sum_i E_{Ti}^{tower} w_i \sin(2\phi_i)}{\sum_i E_{Ti}^{tower} w_i \cos(2\phi_i)}\right), \tag{3}$$

where the sums run over transverse energies, E_T^{tower}, as measured in calorimeter towers located at negative (N) and positive (P) η in the first sampling layer of the FCal. The FCal towers consist of cells grouped into projective regions in $\Delta\eta \times \Delta\phi$ of 0.1×0.1. The weights, $w_i(\Delta\eta_i, \Delta\phi_i)$ are used to correct for any non-uniformity in the event-averaged azimuthal angle distribution of E_T^{tower}. They are determined from the data in narrow $\Delta\eta_i$ and $\Delta\phi_i$ slices.

In the sub-event approach, potential non-flow correlations are minimized by using the reaction plane estimated from the η side opposite to the tracks used for the v_2 measurement; this provides a separation of $\Delta\eta > 3.2$. This method was previously applied [18] to measure v_2 as a function of p_T using charged-particle tracks reconstructed in the ID tracking system with a minimum p_T of 0.5 GeV.

In order to perform the integration over p_T, the differential v_2 measurements are weighted by the number of charged-particle tracks $N_{i,k}^{corr}$,

$$v_2 = \sum_i \sum_k v_2(\eta_i, p_{T,k}) N_{i,k}^{corr} / \sum_i \sum_k N_{i,k}^{corr}, \tag{4}$$

and summed over bins in η (denoted by the index i) and p_T (index k). The number of charged-particle tracks is calculated as $N_{i,k}^{corr} = N_{i,k}[1 - f(i,k)]/\epsilon(i,k)$, where the $N_{i,k}$ is the observed number of tracks in a given η and p_T bin, $\epsilon(i,k)$ is the track reconstruction efficiency and $f(i,k)$ is the estimated rate of fake tracks. In the following sections, the lower limit in the integration of v_2 over p_T is denoted by $p_{T,0}$.

5 Track reconstruction

The ID was used to reconstruct charged-particle trajectories. Three track reconstruction methods were applied in order to exploit a large range in particle p_T:

– the tracklet (TKT) method used for the field-off data in order to reach charged-particle p_T below 0.1 GeV [28],
– the pixel track (PXT) method used to reconstruct tracks with $p_T \geq 0.1$ GeV using only the pixel detector in the field-on data sample,
– the ID track (IDT) method for the field-on data sample, the default ATLAS reconstruction method, for which all ID sub-detectors are used and the track p_T is limited to $p_T \geq 0.5$ GeV [29].

In the TKT method for field-off data, tracks are formed from the positions of hit clusters in the inner two layers of the pixel detector and the position of the primary vertex reconstructed using ID tracks. In the first step, the η_0 and ϕ_0 coordinates are defined using the event's vertex position and the hit recorded in the first pixel layer. Then a search for a hit in the second pixel layer (with η_1 and ϕ_1 coordinates defined with respect to the vertex position) is performed and its consistency with a straight-track hypothesis is checked. Candidate tracklets are required to satisfy the condition

$$\Delta R = \frac{1}{\sqrt{2}}\sqrt{\left(\frac{\Delta\eta}{\sigma_\eta(\eta_0)}\right)^2 + \left(\frac{\Delta\phi}{\sigma_\phi(\eta_0)}\right)^2} < N_\sigma, \tag{5}$$

where $\Delta\eta = \eta_1 - \eta_0$ and $\Delta\phi = \phi_1 - \phi_0$, and $\sigma_\eta(\eta_0)$ and $\sigma_\phi(\eta_0)$ are pseudorapidity-dependent widths of the $\Delta\eta$ and $\Delta\phi$ distributions, respectively. In this analysis, $N_\sigma = 3$ was used as the default condition. Clusters located close to each other in the second pixel layer are most likely to originate from the same particle. Therefore, if more than one cluster located in the second pixel layer fulfils the selection criteria, the resulting tracklets are merged into a single tracklet. The $\Delta\eta$ and $\Delta\phi$ distributions in data and MC simulation are compared in Fig. 1. The data and MC distributions agree well. Candidates fulfilling the criterion in Eq. (5) were accepted for further analysis with $\eta = \eta_0$ and $\phi = \phi_0$.
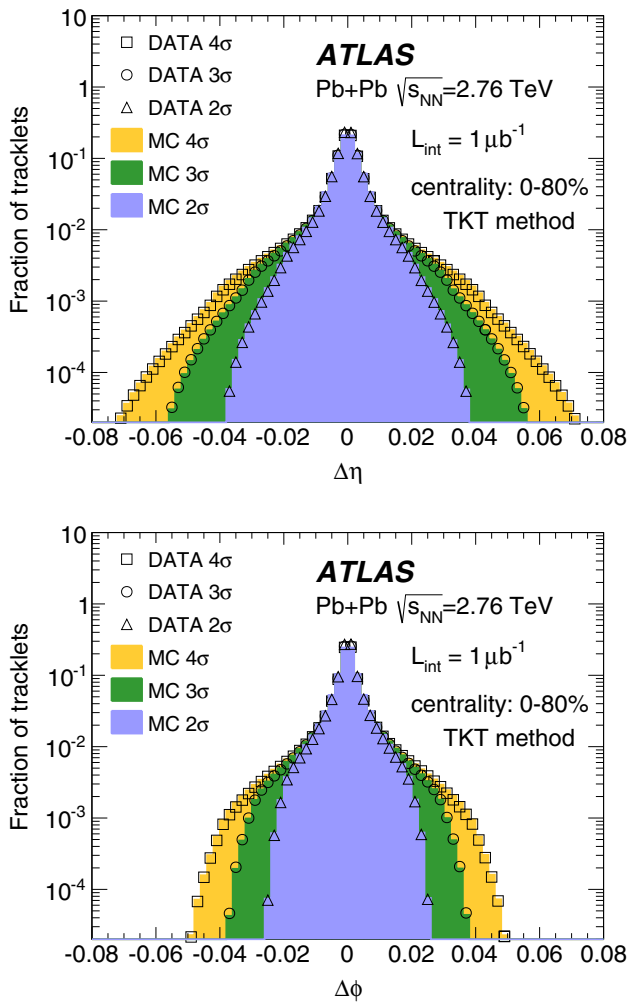
Fig. 1 Comparison of the tracklets' $\Delta\eta$ (*top*) and $\Delta\phi$ (*bottom*) distributions in data (*open symbols*) and MC simulation (*filled histograms*) for tracklets measured within the pseudorapidity range $|\eta| < 2$, for events in the 0–80 % centrality interval and $\Delta R < 4\sigma$, 3σ and 2σ (see Sect. 5 for details) as described in the legend

Fig. 2 Monte Carlo evaluation of the tracklet reconstruction performance in representative centrality bins 0–10, 40–50 and 70–80 %. *Left* generator-level transverse momentum distributions of primary charged particles, N_{primary} (*open circles*), compared to the p_T spectra of charged particles matched to the reconstructed tracklets, N_{matched} (*red triangles*). *Bottom panels* show the ratios of the two distributions. *Right* pseudorapidity, η, dependence of the ratio of all reconstructed tracklets, N_{reco} (*open circles*), and N_{matched} (*red triangles*) to all primary charged particles. The ratio of fake tracklets, N_{fake} (*grey diamonds*), to all reconstructed tracklets is also shown

This method does not provide information about the track's p_T; nevertheless, its performance can be checked as a function of generator-level particle p_T by applying the same reconstruction procedure to the MC simulation and using the p_T of the generated particle corresponding to the reconstructed tracklet whenever applicable. Figure 2 compares the p_T spectra of stable charged particles at the MC-generator level, N_{primary}, to the spectra of reconstructed tracklets matched to charged particles, N_{matched}, for three representative centrality bins and for $|\eta| < 1$. A particle was considered to be primary if it originated directly from the collision or resulted from the decay of a particle with $c\tau < 1$ mm. The matching criterion required that the two hits forming the tracklet be identical to the hits associated with a charged particle. The distributions show that the TKT method is able to reconstruct particles with transverse
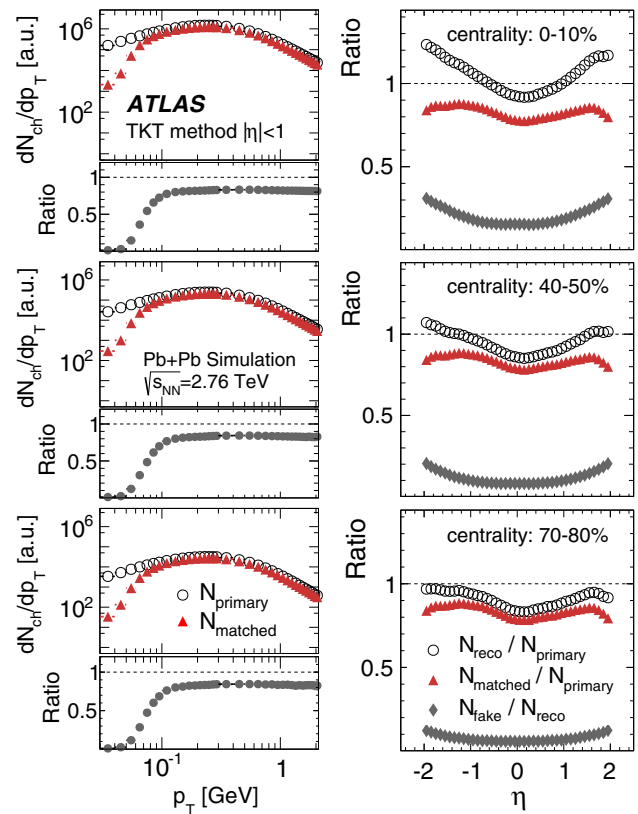
momenta ~ 0.07 GeV with 50 % efficiency, and that a plateau at about 80 % is reached for $p_T > 0.1$ GeV in all centrality bins. For low p_T, the efficiency decreases sharply, but the particle density is small in this region, as is v_2; thus the contribution from this region to the integrated elliptic flow is expected to be small. Figure 2 also shows the reconstruction efficiency, $N_{\text{matched}}/N_{\text{primary}}$, as a function of η. Here, N_{primary} denotes all primary charged particles with $p_T \geq 0.07$ GeV, which defines the low-p_T limit for integrating v_2 over p_T. The efficiency is found to be ~ 80 % and depends weakly on η. The rate of fake tracklets, N_{fake}, measured as the ratio of the number of tracklets not matched to charged particles to the total number of reconstructed tracklets, $N_{\text{fake}}/N_{\text{reco}}$, increases with centrality and $|\eta|$, reaching about 35 % for the most central collisions at $|\eta| = 2$. For field-on data, the PXT method allows the transverse momentum range $p_T > 0.1$ GeV to be examined. Tracks were reconstructed within the full acceptance of the pixel detector ($|\eta| < 2.5$).
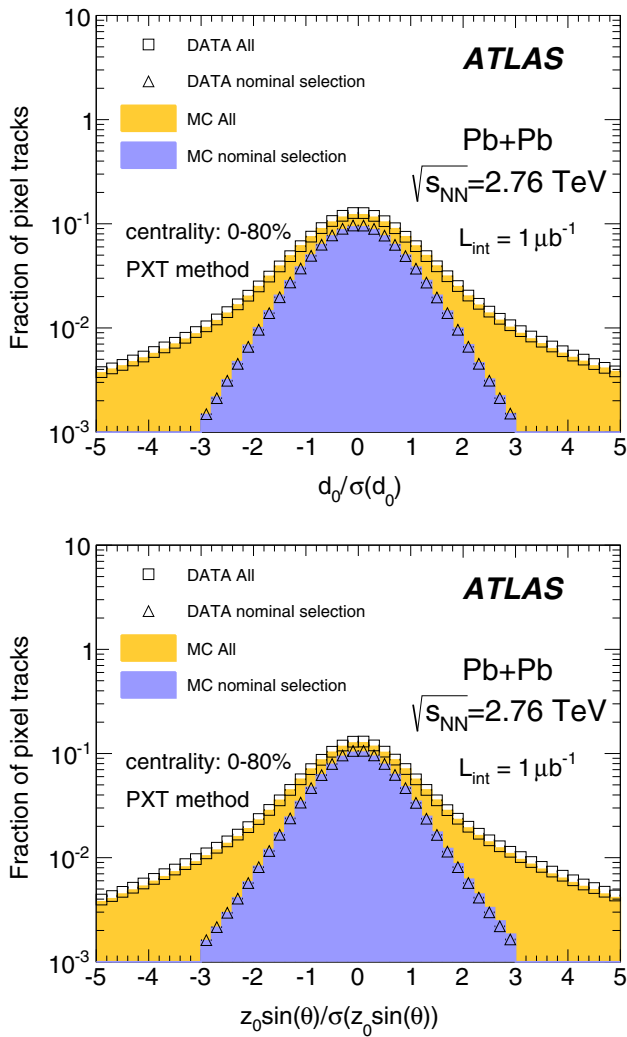
Fig. 3 Comparison of distributions of the transverse (*top*), and longitudinal (*bottom*) impact parameter significances in data and MC simulation for all reconstructed tracks and for the selected tracks (see text for details)

Fig. 4 The transverse momentum, p_T, dependence of the pixel track reconstruction efficiency (*left*) and the fake rate (*right*) for three pseudorapidity ranges and three centrality intervals as indicated in the legend

To improve the track reconstruction's performance in the heavy-ion collision environment, the track-quality requirements were made more stringent than those for proton–proton collisions [30]. Pixel tracks were required to have no missing hits in the pixel layers, and the transverse and longitudinal impact parameters, d_0 and z_0, with respect to the vertex were required to have $|d_0|$ and $|z_0 \sin(\theta)|$ less than 1 mm and significances $|d_0/\sigma_{d_0}|$ and $|z_0 \sin\theta/\sigma_{z_0 \sin\theta}|$ less than 3.0. Figure 3 shows good agreement between data and MC simulation in the distributions of $|d_0/\sigma_{d_0}|$ and $|z_0 \sin\theta/\sigma_{z_0 \sin\theta}|$.

The pixel track method's reconstruction efficiency was evaluated in MC simulation by matching reconstructed tracks to the generated charged particles. A track is matched to a generated charged particle if it is reconstructed from at least 69 % of the pixel hits originating from the latter. Figure 4 illustrates the dependence of the pixel track recon-
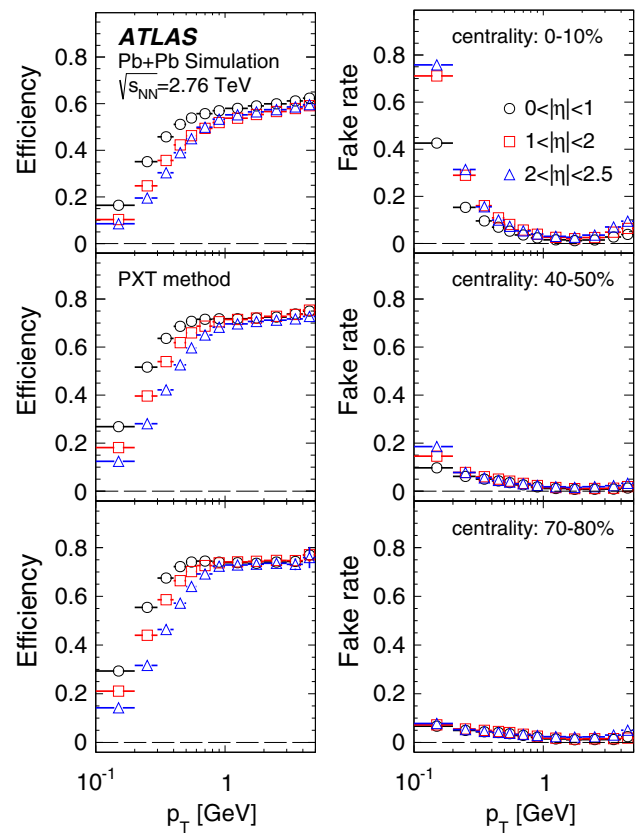
struction efficiency on p_T in three pseudorapidity ranges and for three selected centrality bins. The efficiency decreases slightly from peripheral to central collisions and also deteriorates when moving away from mid-rapidity. A weak p_T dependence is observed above $p_T > 0.5$ GeV for all collision centralities. At lower p_T, the efficiency decreases with decreasing p_T and to about 20 % at the lowest accessible p_T.

The fraction of fake tracks, defined as the ratio of reconstructed tracks not matched to generated charged particles to all reconstructed pixel tracks, was evaluated using MC simulation. Figure 4 shows the fake-rate dependence on p_T in three pseudorapidity ranges and for three centrality bins. The fake rate is below 10 % for p_T above 0.4 GeV and depends very weakly on p_T and η for peripheral collisions. In more central collisions, the fake rate increases at low p_T and shows a similar increase with increasing $|\eta|$.

The performance of the PXT reconstruction method can be compared with that of the IDT method. The track reconstruction efficiency and rate of fake tracks from the IDT method are shown in Fig. 5 (for reconstruction details see Ref. [18]). The minimum p_T reached is 0.5 GeV. A comparison of Figs. 4 and 5 shows that the extension towards lower
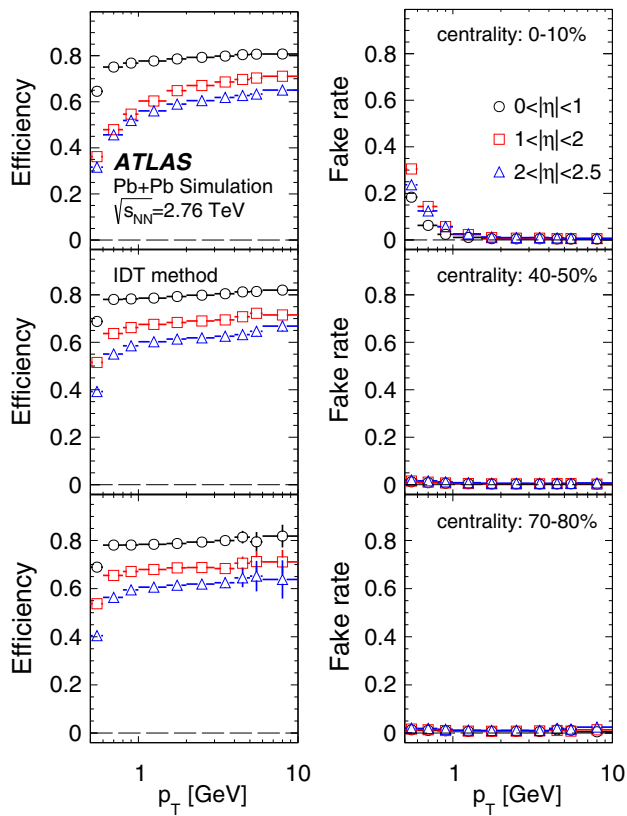
Fig. 5 The transverse momentum, p_T, dependence of the ID track reconstruction efficiency (*left*) and the fake rate (*right*) for three pseudorapidity ranges and three centrality intervals as indicated in the legend

Fig. 6 Comparison of the distribution of multiplicity ratios of number of tracklets, N_{TKT}, (*left*) and pixel tracks, N_{PXT}, (*right*) to the number of ID tracks, N_{IDT}, in data (*red*) and MC simulation (*blue*) in three centrality bins as indicated on the plots

p_T values for the PTX method is achieved at the expense of much larger fake rates than observed for the IDT method, whereas the reconstruction efficiencies are similar. The two methods have different p_T resolutions: it is very good for ID tracks, the root mean square of ($p_T^{reco}/p_T^{true} - 1$) being, in $|\eta| < 1$, about 4 % and independent of the track p_T in the used range, whereas for pixel tracks it is about 10 % at the lowest p_T and increases to about 15 % at 5 GeV.

The performance of the MC simulation in describing the fake rates in the data was checked by comparing the $\Delta\eta$, $\Delta\phi$, d_0/σ_{d_0} and $z_0 \sin\theta/\sigma_{z_0 \sin\theta}$ distributions, like the ones shown in Figs. 1 and 3. Additionally, the distributions of the ratios of the number of tracklets and pixel tracks to the number of ID tracks in data and MC simulation were compared, as shown in Fig. 6. It can be concluded that the MC description of the TKT and PXT methods' performance is adequate.

The elliptic flow depends on the particle type [31] as does the reconstruction efficiency. Although the track reconstruction efficiency is averaged over all particle types in this analysis, the reconstruction efficiencies for simulated pions, kaons and protons are shown as a function of p_T in the Appendix. At low transverse momenta, which are the focus of this analysis, the measured v_2 is dominated by pions with negligi-
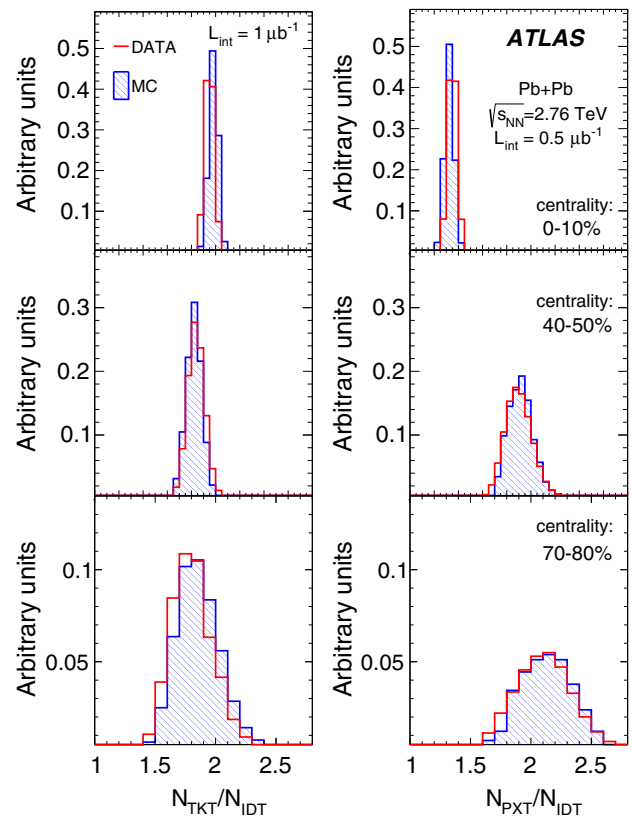
ble contributions from kaons and protons. Nevertheless, the information on the particle type-dependent efficiencies can be used for detailed comparison of the measurement to theoretical predictions of the elliptic flow for identified particles.

6 Corrections to measured v_2

The event-plane method [3] is applied to measure the differential elliptic flow harmonic $v_2(\eta)$ in small η bins with the TKT method, and $v_2(\eta, p_T)$ in small η and p_T bins with the PXT and IDT methods. The differential v_2 measurements are then corrected for detector-related effects.

The first correction is associated with the variation in tracking efficiency induced by the flow itself. It is applied only to the PXT method, which is found to be sensitive to the detector occupancy. Such sensitivity is not observed for the IDT method. Since the flow phenomenon is a modulation of the multiplicity, it may induce a variation of the tracking efficiency in an event. Higher occupancy causes lower efficiency, and the number of tracks observed in the event plane is reduced more strongly than the number of tracks observed in other directions. As a consequence, the observed

v_2 is smaller. In order to correct for this effect, an appropriate weight was applied to the tracks in the calculation of the numerator of Eq. (2). This weight, the inverted efficiency parameterized as a function of detector occupancy in the vicinity of the track, was derived from MC simulation. In the data, the occupancy was determined for each track from the number of hits near the track in the first layer of the pixel detector. The corrected $v_2(p_T)$ was compared to the measurement obtained from the IDT method in the same data. In the MC simulation, the comparison was made to $v_2(p_T)$ determined using generated particles. The relative increases in the value of $v_2(p_T)$ in data and in simulation were found to be compatible for $p_T > 0.5$ GeV, the range in which the comparison could be performed.

The occupancy correction results in an increase of about 12 % in the integrated v_2 for the 0–20 % centrality interval while it amounts to only 1 % for the most peripheral collisions, when using a lower p_T integration limit of $p_{T,0} = 0.1$ GeV. For higher values of $p_{T,0}$ the correction gradually becomes smaller. For $p_{T,0} = 0.5$ GeV it decreases to about 7 % for the most central collisions.

An additional correction, applied to the differential measurement of v_2, accounts for the difference between v_2 measured only with fake tracks and v_2 measured with charged-particle tracks from the primary vertex. The corrected v_2 is calculated as

$$v_2 = \frac{v_{2,m} - f v_{2,f}}{1 - f}, \tag{6}$$

where $v_{2,m}$ is the elliptic flow measured with all tracks, $v_{2,f}$ is the flow of fake tracks, and f is the fake-track rate. This correction was applied to the differential v_2 measured with the TKT, PXT and IDT methods with the corresponding fake rates and $v_{2,f}$ values. The rate and $v_{2,f}$ of the fake tracks were derived from MC simulation and then cross-checked in the data with a sample, obtained with inverted track selection criteria, in which fake tracks dominate. Differences between the MC simulation and the data of up to 20 % were observed and included in the systematic uncertainties.

The fake tracks reduce the values of v_2 integrated over the p_T ranges considered in this analysis. The correction is a function of the fake-track rate and accordingly exhibits a dependence on centrality, p_T and η. For $|\eta| < 1$, the largest correction, about 15 %, was obtained for the PXT method with $p_{T,0} = 0.1$ GeV. For peripheral collisions in the same kinematic range, it decreases to about 11 %. The correction is smaller for higher values of $p_{T,0}$. It decreases to about 2 % for $p_{T,0} = 0.5$ GeV for the 0–10 % centrality interval and gradually drops to zero for the most peripheral collisions. The fake-track flow correction for the integrated v_2 obtained with the IDT method ($p_{T,0} = 0.5$ GeV) is less than 2 % for the most central collisions and even smaller for the more

peripheral ones. For the TKT method, the correction is about 1 % for the most central collisions.

The limited p_T resolution for tracks reconstructed in the pixel detector and the rapidly changing dN_{ch}/dp_T distribution lead to a significant bin-to-bin migration in p_T. As a consequence of the variation of v_2 with p_T, v_2 measured in a given p_T bin is contaminated by v_2 values of particles from the neighbouring bins. In order to compensate for this effect, a correction derived from MC simulation was applied to the $v_2(p_T)$ values. This correction was determined, using pixel tracks matched to generated particles, by comparing the $v_2(p_T)$ distribution as a function of reconstructed p_T to $v_2(p_T)$ as a function of generated p_T. In order to validate the correction derived from the MC simulation, the same procedure was applied in the data and in the simulation in the region of $p_T > 0.5$ GeV , where the ID tracks were used instead of the generated particles. The ID tracks were matched by requiring an angular separation $\sqrt{(\Delta\eta)^2 + (\Delta\phi)^2} < 0.02$. A comparison between the corrections obtained in the data and in the MC simulation, as a function of measured p_T, showed a good agreement.

The correction for p_T-bin migration of the reconstructed tracks was found to be small compared to the occupancy and fake-track flow corrections, and to depend only on the value of $p_{T,0}$. It increases the integrated v_2 value by 1 % (1.5 %) for $p_{T,0} = 0.1$ GeV ($p_{T,0} = 0.5$ GeV) independently of collision centrality.

## 7 Uncertainties in the v_2 determination

The systematic uncertainties include those common to different tracking methods, as well as method-specific ones.

The uncertainty which originates from the statistics of the MC samples is treated as a source of systematic uncertainty.

The v_2 values determined for samples enriched in fake tracks in data and MC simulation were compared and differences of up to 20 % for both the PXT and IDT methods were observed. For the PXT method, this difference resulted in a change of v_2, integrated from $p_{T,0} = 0.1$ GeV, for the most central (0–10 %) collisions of 3 % at mid-rapidity and of 15 % at $|\eta| \sim 2$. The impact on the integrated v_2 decreases with increasing centrality. For higher $p_{T,0}$ values, the change was found to be negligible. For the IDT method, the uncertainty on the v_2 value of fake tracks induces a systematic uncertainty in the integrated v_2 for central collisions of less than 4 % at mid-rapidity and of 9 % at $|\eta| \sim 2$; for peripheral collisions the uncertainty is smaller.

The variation of the fake tracklets' v_2, at the level of 10 %, obtained from the comparison of data and MC simulation, results in an uncertainty at the level of 2 % in the integrated v_2 across the centrality range 0–40 %.

Fig. 7 Contributions to the relative systematic uncertainty on the elliptic flow, $\Delta v_2/\langle v_2\rangle$, as a function of centrality for $|\eta| < 1$ with the TKT (*left*), PXT (*centre*) and IDT (*right*) methods. The integration limits for the three methods are 0.07, 0.1, 0.5 GeV, respectively. The total uncertainty is indicated by the *shaded area*. The individual contributions, are described in the legend and explained in the text
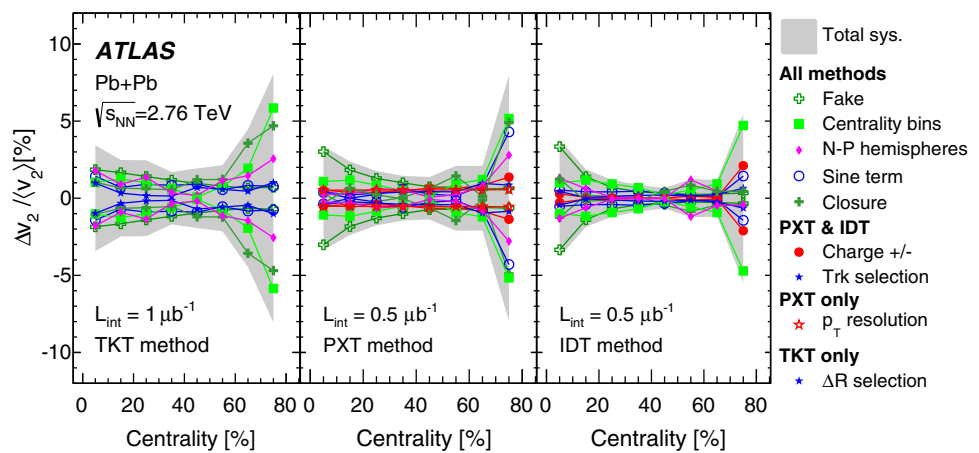
A comparison of v_2 values obtained with the TKT method for a MC sample with the nominal detector geometry to that with 10 % more active material and 15–20 % more inactive material shows agreement to better than 2 %. Therefore it was assumed that possible inaccuracies in the description of the detector material in the GEANT4 simulation have a negligible effect on the final results. The same holds for the measurements with the PXT and IDT methods.

An overall scale uncertainty on v_2 originates from the uncertainty on the fraction of the total inelastic cross section accepted by the trigger as well as from the event selection criteria, which affects the population of the centrality bins. It is negligibly small (below 1 %) for central collisions and increases to about 6 % for the most peripheral collisions for the TKT method and to about 5 % for both the PXT and IDT methods.

The influence of the detector nonuniformities on the measured v_2 was checked by comparing the v_2 values obtained for positive and negative η. This led to a typical uncertainty of 1 % except for the most peripheral collisions where it increased to about 2 %.

Deviations of $\langle\sin 2[\phi - \Psi_2]\rangle$ from zero point to detector non-uniformities and biases in the event-plane determination. The magnitude of the sine term relative to the cosine term is included in the systematic uncertainty of v_2. For the TKT method, its contribution to the relative systematic uncertainty is negligibly small. For the PXT and IDT methods, it is small for most centrality bins, and increases to 2 % only for the most peripheral collisions.

The analysis procedure was checked with MC studies in which the generated elliptic flow signal was compared to the v_2 values obtained with the same analysis chain as used for the data. In this MC closure test, relative differences of up to 2 % in central collisions and of up to 5 % in peripheral collisions were observed for the TKT method. For the IDT method, the relative difference reaches 2 %; for the PXT method, it remains within 2 % except for the most peripheral

collisions where it increases to 5 %. The relative difference between the expected and measured values is included in the total systematic uncertainty.

The ΔR parameter used in the tracklet reconstruction was varied by $\pm 1\sigma$ from the nominal value. The resulting variation in the value of v_2 at the level of 1 % is included in the systematic uncertainty. For the PXT and IDT methods, differences between v_2 determined from tracks of negatively and positively charged particles as well as between the baseline v_2 and that obtained with tighter or looser tracking requirements (in which the transverse and longitudinal impact parameter significance criteria are changed by ± 1) also contribute to the systematic uncertainty at the level of a few percent.

For the PXT method, the corrections due to the limited p_T resolution were varied within their statistical uncertainties and the resulting variation was found to be at the level of 0.5 %, independently of the centrality.

The p_T spectrum of charged particles in the MC simulation was reweighted so that the expected detector-level distribution agrees with that observed in the data. This changes the effective fake-track rate and therefore the weights used in the calculation of v_2. A variation of these weights by up to 10 % has a negligible effect on the determination of v_2.

The different contributions to the total systematic uncertainty on the integrated v_2 for $|\eta| < 1$ are shown in Fig. 7 and summarized in Table 1 for the three tracking methods. The total systematic uncertainties are determined by adding in quadrature all the individual contributions and are treated as $\pm 1\sigma$ uncertainties.

8 Results

Figure 8 shows the centrality dependence of v_2 integrated over $|\eta| < 1$. For the TKT method, v_2 is integrated over $p_T > 0.07$ GeV. For the PXT method, v_2 is integrated over $p_{T,0} < p_T < 5$ GeV and $p_{T,0}$ is varied from 0.1 to 0.5 GeV in steps

Table 1 Summary of the systematic uncertainties as percentages of the integrated v_2 value for charged particles with $|\eta| < 1$ and different collision centrality bins

Source	Centrality bin				
	0–10 %	10–20 %	20–60 %	60–70 %	70–80 %
TKT $p_T > 0.07$ GeV					
MC Statistics	0.1	0.1	<0.2	0.3	1
Fake tracks	2	2	1–2	1	1
Centrality bins	1	1.5	<1	2	6
N-P η regions	2	1	<1.5	1	2.5
Sine term	1.5	1	1	1	1
Closure	1.5	1	<2	3.5	5
ΔR	1	0.5	<1	0.5	1
Total	3.5	3.2	<3.2	4	8
PXT $p_T > 0.1$ GeV					
MC Statistics	0.1	0.1	<0.2	0.3	1
Fake tracks	3	2	<1.5	0.5	0.5
Centrality bins	1	1.5	<1	1.5	5
N-P η regions	0.5	0.5	<0.5	1	3
Sine term	0.5	0	<0.5	1	4
Closure	1	1	<2	0	5
Charge $\pm$	0.5	0.5	<1	1	1.5
Track selection	0.5	0.5	<0.5	1	1
p_T resolution	0.5	0.5	0.5	0.5	0.5
Total	3	2	<2	2	8
IDT $p_T > 0.5$ GeV					
MC Statistics	0.1	0.1	<0.2	0.3	1
Fake tracks	3.5	1.5	<1	0.2	0.2
Centrality bins	1	1.5	<1	1	5
N-P η regions	1.2	1	<1.5	0.5	0.5
Sine term	0.5	0.5	0.5	0.5	1.5
Closure	1.5	0.5	<1	0.5	0.5
Charge $\pm$	0.2	0.2	0.2	0.2	2.2
Track selection	0.5	0	<0.5	0.2	1
Total	3.5	2	<1.5	1	5.5

of 0.1 GeV. Also shown is the v_2 value obtained from the IDT method integrated over $0.5 < p_T < 5$ GeV. The TKT method with $p_{T,0} = 0.07$ GeV gives results consistent with the v_2 values obtained with the PXT method with $p_{T,0} = 0.1$ GeV, as could be expected due to the very low charged-particle density and small v_2 signal in the momentum range below 0.1 GeV. This indicates that there is no need to extrapolate the measurements obtained with tracklets down to $p_T = 0$ in order to obtain a reliable estimate of v_2 integrated over the whole kinematic range in p_T. Furthermore, for the PXT method such an extrapolation would result in a very small correction to the measured integrated flow, well within the uncertainties of the measurement. This is in contrast to the integrated v_2 with $p_{T,0}$ chosen at higher values, as also shown

in Fig. 8. It can be seen that the integrated v_2 increases almost linearly with $p_{T,0}$ for $p_{T,0} > 0.1$ GeV. Good agreement between the PXT and IDT methods is observed at $p_{T,0} = 0.5$ GeV. In Fig. 9, the results of this analysis are compared to the integrated v_2 measured by CMS [20] with $p_{T,0} = 0.3$ GeV. In this comparison, the sensitivity to $p_{T,0}$ is clearly visible. A systematically larger v_2 is observed for the higher value of $p_{T,0}$ as a consequence of the strong increase of v_2 with increasing p_T.

The η dependence of the p_T-integrated v_2 provides useful constraints on the initial conditions of heavy-ion collisions used in model descriptions of the system's evolution (see, e.g., Refs. [1,2]). Figure 10 shows the η dependence of the p_T-integrated v_2. As already shown in Fig. 9, the differ-
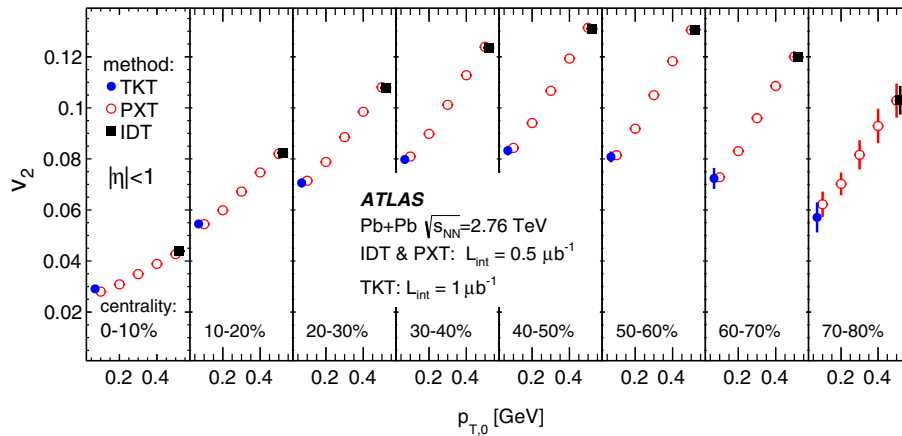
Fig. 8 Elliptic flow v_2 integrated over transverse momentum $p_T > p_{T,0}$ as a function of $p_{T,0}$ for different centrality intervals, obtained with different charged-particle reconstruction methods: the tracklet (TKT) method with $p_{T,0} = 0.07$ GeV, the pixel track (PXT) method with $p_{T,0} \geq 0.1$ GeV and the ID track (IDT) method with $p_{T,0} = 0.5$ GeV as described in the legend. *Error bars* show statistical and systematic uncertainties added in quadrature
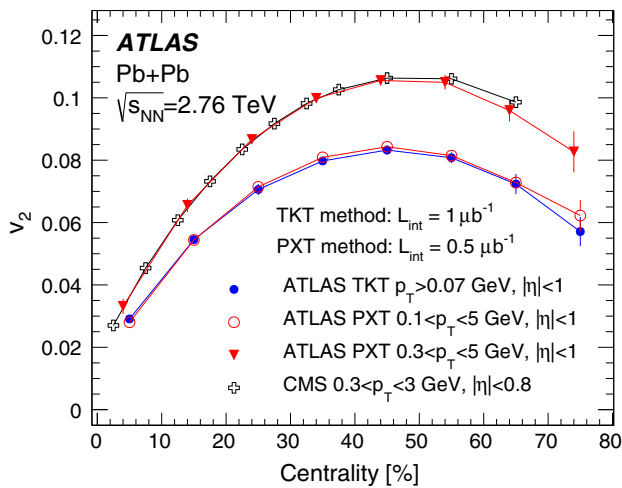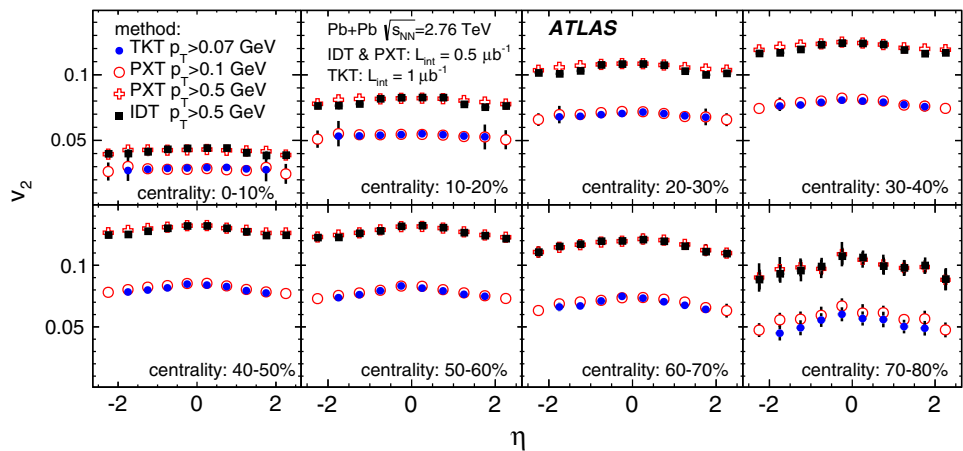

Fig. 9 Centrality dependence of elliptic flow, v_2, measured for $|\eta| < 1$ and integrated over transverse momenta, p_T, for different charged-particle reconstruction methods as described in the legend. Also shown are v_2 measurements by CMS integrated over $0.3 < p_T < 5$ GeV and $|\eta| < 0.8$ [20] (*open crosses*). *Error bars* show statistical and systematic uncertainties added in quadrature

ence between the results obtained with $p_{T,0}$ values of 0.07 and 0.1 GeV is very small and the two measurements agree within uncertainties. The results obtained using the PXT and IDT methods for the same $p_{T,0}$ are also consistent. The η dependence of the integrated v_2 is very weak. A decrease with increasing $|\eta|$ of about 5–10 % is seen. A comparison with the results from the CMS experiment [20] is shown in Fig. 11 for the 40–50 % centrality interval. The ATLAS measurements performed with the PXT method were integrated over p_T for different $p_{T,0}$ values, including one adjusted to match that used by CMS. The results agree, within uncertainties, provided the same $p_{T,0}$ is used.

The different upper limits in the p_T integration, 3 GeV for CMS and 5 GeV for ATLAS, have negligible effect on the integrated v_2 value. A systematic decrease in v_2 with decreasing $p_{T,0}$ is observed as expected from the linear dependence of v_2 on p_T for $p_T \approx 0$. The decreasing value of $p_{T,0}$ together with that of v_2 makes the integration over the full p_T range less sensitive to the uncertainties in the extrapolation down to $p_T = 0$.

Fig. 10 Pseudorapidity, η, dependence of elliptic flow, v_2, integrated over transverse momentum, p_T, for different charged particle reconstruction methods and different low-p_T thresholds in different centrality intervals as indicated in the legend. *Error bars* show statistical and systematic uncertainties added in quadrature
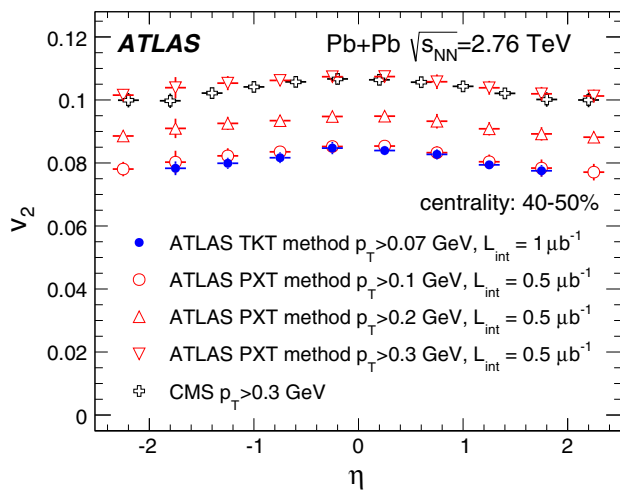
Fig. 11 Comparison of the pseudorapidity, η, dependence of elliptic flow, v_2, integrated over transverse momentum, p_T, for different low-p_T thresholds, as indicated in the legend, in the 40–50 % centrality interval from the ATLAS and CMS experiments. *Error bars* show statistical and systematic uncertainties added in quadrature

The large acceptance in η of the ATLAS and CMS experiments makes it possible to study whether the observation of the extended longitudinal scaling of v_2, when viewed in the rest frame of one of the colliding nuclei, reported by the PHOBOS experiment at RHIC [6,32], holds at the much higher LHC energy. The PHOBOS measurements of elliptic flow over a range of Au+Au collision energies, $\sqrt{s_{NN}} = 19.6, 62.4, 130$ and 200 GeV, showed energy independence of the integrated v_2 as a function of $|\eta| - y_{beam}$, where $y_{beam} = \ln{(\sqrt{s_{NN}}/m)}$ is the beam rapidity and m is the proton mass. A similar effect was also observed in charged-particle densities [6] and is known as limiting fragmentation [33]. In Fig. 12, the integrated v_2 is plotted as a function of $|\eta| - y_{beam}$ and compared to the PHOBOS results for three centrality bins matching those used by PHOBOS. The PHOBOS results are obtained with the event-plane method for

charged particles with a low-p_T limit of 0.035 GeV at mid-rapidity and of 0.004 GeV around the beam rapidity [34]. The CMS data [20] obtained with the event-plane method are also shown. The CMS measurement represents v_2 integrated over p_T from 0 to 3 GeV. This measurement was obtained by extrapolating $v_2(p_T)$ measured for $p_T > 0.3$ GeV and the charged-particle spectra down to $p_T = 0$ under the assumption that $v_2(p_T = 0) = 0$ and with the charged-particle yield constrained by the measured $dN_{ch}/d\eta$ distribution [35]. The ATLAS and CMS results agree within the uncertainties, although the CMS v_2 is systematically smaller by about 5 % than the ATLAS measurement. This small systematic difference can be attributed to the uncertainty in the CMS extrapolation to $p_T = 0$ or the p_T threshold of 0.07 GeV for the ATLAS measurement, or the combination of both.

As can be seen from the figure, there is no overlap in $|\eta| - y_{beam}$ between the PHOBOS and LHC data, so a direct comparison with the low-energy data is not possible. Nevertheless, it can be concluded, keeping in mind the relatively large uncertainties in the low-energy results, that the extrapolation of the trend observed at RHIC to the LHC energy appears to be consistent with the LHC measurements, although the dependence on $|\eta| - y_{beam}$ may be weaker at the LHC energy.

9 Summary and conclusions

Measurements of the integrated elliptic flow of charged particles in Pb+Pb collisions at $\sqrt{s_{NN}} = 2.76$ TeV are presented by the ATLAS experiment at the LHC. The elliptic anisotropy parameter v_2 is measured with the event-plane method over a broad range of collision centralities (0–80 %). The kinematic range in pseudorapidity extends out to $|\eta| = 2.5$, and in p_T down to 0.07 GeV. This low-p_T region is reached by using a tracklet reconstruction algorithm to analyze about $1\,\mu b^{-1}$ of data taken with the solenoid field turned off. Other

Fig. 12 Integrated elliptic flow, v_2, as a function of $|\eta| - y_{beam}$ for three centrality intervals indicated in the legend, measured by the ATLAS and CMS experiments for Pb+Pb collisions at 2.76 TeV and by the PHOBOS experiment for Au+Au collisions at 200 GeV. The CMS result is obtained by averaging the $v_2(p_T)$ with the charged particle spectra over the range $0 < p_T < 3$ GeV. *Error bars* show statistical and systematic uncertainties added in quadrature
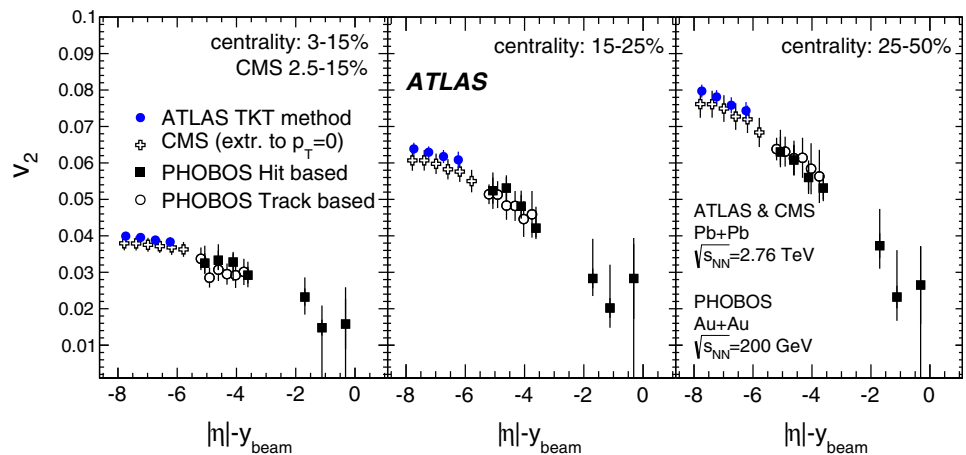
track reconstruction methods with low-p_T thresholds of 0.1 and 0.5 GeV respectively, are exploited in order to verify the tracklet measurement and provide results that can be directly compared to other LHC measurements. The value of v_2 integrated from $p_T = 0.07$ GeV provides a reliable estimate of the elliptic flow measured over the range $p_T \geq 0$.

The p_T-integrated elliptic flow as a function of collision centrality shows a clear dependence on $p_{T,0}$, both within the present measurements and in comparison to the CMS results obtained with higher low-p_T limits. The integrated elliptic flow increases with centrality, reaching a maximum of 0.08 for mid-central collisions (40–50 %) and then decreases to about 0.02 for the most central collisions.

The pseudorapidity dependence of the p_T-integrated v_2 is very weak, with a slight decrease in v_2 as $|\eta|$ increases. The results are in agreement with the CMS measurements covering the same η range, provided the same low-p_T cutoff is used. The integrated v_2 transformed to the rest frame of one of the colliding nuclei is compared to the lower-energy RHIC data. Although a direct comparison is not possible due to the non-overlapping kinematic regions, the general trend observed in the RHIC energy regime seems consistent with the LHC measurements, while the latter may have a weaker dependence on pseudorapidity.

Appendix

In the low-p_T region, the track reconstruction efficiency depends strongly on the particle type. This information is important for comparison of measurements with theory predictions in which the elliptic flow depends on the particle type.

The efficiency of the PXT and TKT methods in reconstructing tracks with $|\eta| < 1$ generated as $\pi^\pm$, $K^\pm$, p, and $\bar{p}$ in MC simulation is shown in Fig. 13 as a function of p_T. Large differences in efficiency are observed for the PXT method at p_T below about 1 GeV and for the TKT method at p_T below about 0.4 GeV. Above these values, the reconstruction efficiency is independent of particle type. The efficiency is lowest for p and $\bar{p}$. For the TKT method, which is most relevant at low p_T, the efficiency for reconstructing protons drops to zero below 0.2 GeV.
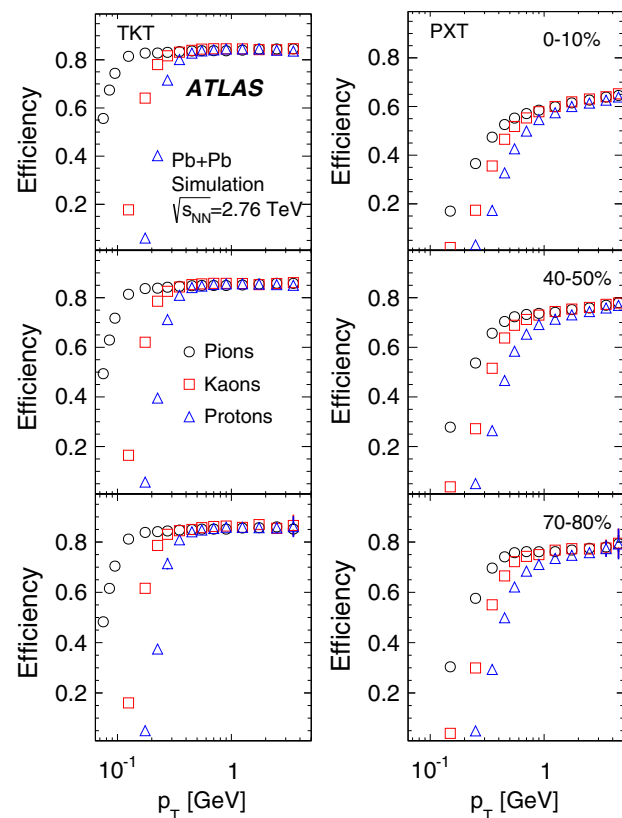

Fig. 13 The transverse momentum, p_T, dependence of the TKT (*left*) and PXT (*right*) track reconstruction efficiency for $\pi^\pm$, $K^\pm$ and $p^\pm$ in the pseudorapidity range $|\eta| < 1$ for three centrality intervals, as indicated in the legend

References

1. P. Romatschke, Int. J. Mod. Phys. E **19**, 1 (2010). arXiv:0902.3663
2. T. Hirano, U.W. Heinz, D. Kharzeev, R. Lacey, Y. Nara, Phys. Lett. B **636**, 299 (2006). arXiv:nucl-th/0511046
3. A.M. Poskanzer, S. Voloshin, Phys. Rev. C **58**, 1671 (1998). arXiv:nucl-ex/9805001
4. ATLAS Collaboration, JHEP **1311**, 183 (2013). arXiv:1305.2942
5. BRAHMS Collaboration, I. Arsene et al., Nucl. Phys. A **757**, 1 (2005). arXiv:nucl-ex/0410020
6. PHOBOS Collaboration, B.B. Back et al., Nucl. Phys. A **757**, 28 (2005). arXiv:nucl-ex/0410022
7. STAR Collaboration, J. Adams et al., Nucl. Phys. A **757**, 102 (2005). arXiv:nucl-ex/0501009
8. PHENIX Collaboration, K. Adcox et al., Nucl. Phys. A **757**, 184 (2005). arXiv:nucl-ex/0410003
9. G. Kestin, U.W. Heinz, Eur. Phys. J. C **61**, 545 (2009). arXiv:0806.4539
10. M. Chojnacki, W. Florkowski, W. Broniowski, A. Kisiel, Phys. Rev. C **78**, 014905 (2008). arXiv:0712.0947
11. P. Romatschke, U. Romatschke, Phys. Rev. Lett. **99**, 172301 (2007). arXiv:0706.1522
12. B.H. Alver, C. Gombeaud, M. Luzum, J.Y. Ollitrault, Phys. Rev. C **82**, 034913 (2010). arXiv:1007.5469
13. U.W. Heinz, J.S. Moreland, H. Song, Phys. Rev. C **80**, 061901 (2009). arXiv:0908.2617
14. H. Song, U.W. Heinz, Phys. Rev. C **81**, 024905 (2010). arXiv:0909.1549
15. Z. Qiu, C. Shen, U.W. Heinz, Phys. Lett. B **707**, 151 (2012). arXiv:1110.3033
16. ALICE Collaboration, K. Aamodt et al., Phys. Rev. Lett. **105**, 252302 (2010). arXiv:1011.3914
17. ALICE Collaboration, K. Aamodt et al., Phys. Rev. Lett. **107**, 032301 (2011). arXiv:1105.3865
18. ATLAS Collaboration, Phys. Lett. B **707**, 330 (2012). arXiv:1108.6018
19. ATLAS Collaboration, Phys. Rev. C **86**, 014907 (2012). arXiv:1203.3087
20. CMS Collaboration, Phys. Rev. C **87**, 014902 (2013). arXiv:1204.1409
21. CMS Collaboration, Phys. Rev. Lett. **109**, 022301 (2012). arXiv:1204.1850
22. B. Schenke, S. Jeon, C. Gale, Phys. Rev. Lett. **106**, 042301 (2011). arXiv:1009.3244
23. P. Bozek, Phys. Rev. C **85**, 034901 (2012). arXiv:1110.6742
24. ATLAS Collaboration, JINST **3**, S08003 (2008)
25. M. Gyulassy, X.N. Wang, Comput. Phys. Commun. **83**, 307 (1994). arXiv:nucl-th/9502021
26. ATLAS Collaboration, Eur. Phys. J. C **70**, 823 (2010). arXiv:1005.4568
27. S. Agostinelli et al., Nucl. Instrum. Methods A **506**, 250 (2003)
28. ATLAS Collaboration, Phys. Lett. B **710**, 363 (2012). arXiv:1108.6027
29. ATLAS Collaboration, Phys. Lett. B **688**, 21 (2010). arXiv:1003.3124
30. ATLAS Collaboration, New J. Phys. **13**, 053033 (2011). arXiv:1012.5104
31. ALICE Collaboration, B. Abelev et al. (2014). arXiv:1405.4632
32. PHOBOS Collaboration, B.B. Back et al., Phys. Rev. C **72**, 051901 (2005). arXiv:nucl-ex/0407012
33. J. Benecke, T.T. Chou, C.N. Yang, E. Yen, Phys. Rev. **188**, 2159 (1969)
34. PHOBOS Collaboration, B.B. Back et al., Phys. Rev. C 74, 021901 (2006). arXiv:nucl-ex/0509034
35. CMS Collaboration, JHEP **1108**, 141 (2011). arXiv:1107.4800

The ATLAS Collaboration

G. Aad[84], B. Abbott[112], J. Abdallah[152], S. Abdel Khalek[116], O. Abdinov[11], R. Aben[106], B. Abi[113], M. Abolins[89], O. S. AbouZeid[159], H. Abramowicz[154], H. Abreu[137], R. Abreu[30], Y. Abulaiti[147a,147b], B. S. Acharya[165a,165b,a], L. Adamczyk[38a], D. L. Adams[25], J. Adelman[177], S. Adomeit[99], T. Adye[130], T. Agatonovic-Jovin[13b], J. A. Aguilar-Saavedra[125a,125f], M. Agustoni[17], S. P. Ahlen[22], F. Ahmadov[64,b], G. Aielli[134a,134b], T. P. A. Åkesson[80], G. Akimoto[156], A. V. Akimov[95], G. L. Alberghi[20a,20b], J. Albert[170], S. Albrand[55], M. J. Alconada Verzini[70], M. Aleksa[30], I. N. Aleksandrov[64], C. Alexa[26a], G. Alexander[154], G. Alexandre[49], T. Alexopoulos[10], M. Alhroob[165a,165b], G. Alimonti[90a], L. Alio[84], J. Alison[31], B. M. M. Allbrooke[18], L. J. Allison[71], P. P. Allport[73], S. E. Allwood-Spiers[53], J. Almond[83], A. Aloisio[103a,103b], A. Alonso[36], F. Alonso[70], C. Alpigiani[75], A. Altheimer[35], B. Alvarez Gonzalez[89], M. G. Alviggi[103a,103b], K. Amako[65], Y. Amaral Coutinho[24a], C. Amelung[23], D. Amidei[88], S. P. Amor Dos Santos[125a,125c], A. Amorim[125a,125b], S. Amoroso[48], N. Amram[154], G. Amundsen[23], C. Anastopoulos[140], L. S. Ancu[49], N. Andari[30], T. Andeen[35], C. F. Anders[58b], G. Anders[30], K. J. Anderson[31], A. Andreazza[90a,90b], V. Andrei[58a], X. S. Anduaga[70], S. Angelidakis[9], I. Angelozzi[106], P. Anger[44], A. Angerami[35], F. Anghinolfi[30], A. V. Anisenkov[108], N. Anjos[125a], A. Annovi[47], A. Antonaki[9], M. Antonelli[47], A. Antonov[97], J. Antos[145b], F. Anulli[133a], M. Aoki[65], L. Aperio Bella[18], R. Apolle[119,c], G. Arabidze[89], I. Aracena[144], Y. Arai[65], J. P. Araque[125a], A. T. H. Arce[45], J-F. Arguin[94], S. Argyropoulos[42], M. Arik[19a], A. J. Armbruster[30], O. Arnaez[82], V. Arnal[81], H. Arnold[48], O. Arslan[21], A. Artamonov[96], G. Artoni[23], S. Asai[156], N. Asbah[94], A. Ashkenazi[154], S. Ask[28], B. Åsman[147a,147b], L. Asquith[6], K. Assamagan[25], R. Astalos[145a], M. Atkinson[166], N. B. Atlay[142], B. Auerbach[6], K. Augsten[127], M. Aurousseau[146b], G. Avolio[30], G. Azuelos[94,d], Y. Azuma[156], M. A. Baak[30], C. Bacci[135a,135b], H. Bachacou[137], K. Bachas[155], M. Backes[30], M. Backhaus[30], J. Backus Mayes[144], E. Badescu[26a], P. Bagiacchi[133a,133b], P. Bagnaia[133a,133b], Y. Bai[33a], T. Bain[35], J. T. Baines[130], O. K. Baker[177], S. Baker[77], P. Balek[128], F. Balli[137], E. Banas[39], Sw. Banerjee[174], A. Bangert[151], A. A. E. Bannoura[176], V. Bansal[170], H. S. Bansil[18], L. Barak[173], S. P. Baranov[95], E. L. Barberio[87], D. Barberis[50a,50b], M. Barbero[84], T. Barillari[100], M. Barisonzi[176], T. Barklow[144], N. Barlow[28], B. M. Barnett[130], R. M. Barnett[15], Z. Barnovska[5], A. Baroncelli[135a], G. Barone[49], A. J. Barr[119], F. Barreiro[81], J. Barreiro Guimarães da Costa[57], R. Bartoldus[144], A. E. Barton[71], P. Bartos[145a], V.

Bartsch[150], A. Bassalat[116], A. Basye[166], R. L. Bates[53], L. Batkova[145a], J. R. Batley[28], M. Battistin[30], F. Bauer[137], H. S. Bawa[144,e], T. Beau[79], P. H. Beauchemin[162], R. Beccerle[123a,123b], P. Bechtle[21], H. P. Beck[17], K. Becker[176], S. Becker[99], M. Beckingham[139], C. Becot[116], A. J. Beddall[19c], A. Beddall[19c], S. Bedikian[177], V. A. Bednyakov[64], C. P. Bee[149], L. J. Beemster[106], T. A. Beermann[176], M. Begel[25], K. Behr[119], C. Belanger-Champagne[86], P. J. Bell[49], W. H. Bell[49], G. Bella[154], L. Bellagamba[20a], A. Bellerive[29], M. Bellomo[85], A. Belloni[57], K. Belotskiy[97], O. Beltramello[30], O. Benary[154], D. Benchekroun[136a], K. Bendtz[147a,147b], N. Benekos[166], Y. Benhammou[154], E. Benhar Noccioli[49], J. A. Benitez Garcia[160b], D. P. Benjamin[45], J. R. Bensinger[23], K. Benslama[131], S. Bentvelsen[106], D. Berge[106], E. Bergeaas Kuutmann[16], N. Berger[5], F. Berghaus[170], E. Berglund[106], J. Beringer[15], C. Bernard[22], P. Bernat[77], C. Bernius[78], F. U. Bernlochner[170], T. Berry[76], P. Berta[128], C. Bertella[84], F. Bertolucci[123a,123b], M. I. Besana[90a], G. J. Besjes[105], O. Bessidskaia[147a,147b], N. Besson[137], C. Betancourt[48], S. Bethke[100], W. Bhimji[46], R. M. Bianchi[124], L. Bianchini[23], M. Bianco[30], O. Biebel[99], S. P. Bieniek[77], K. Bierwagen[54], J. Biesiada[15], M. Biglietti[135a], J. Bilbao De Mendizabal[49], H. Bilokon[47], M. Bindi[54], S. Binet[116], A. Bingul[19c], C. Bini[133a,133b], C. W. Black[151], J. E. Black[144], K. M. Black[22], D. Blackburn[139], R. E. Blair[6], J.-B. Blanchard[137], T. Blazek[145a], I. Bloch[42], C. Blocker[23], W. Blum[82,*], U. Blumenschein[54], G. J. Bobbink[106], V. S. Bobrovnikov[108], S. S. Bocchetta[80], A. Bocci[45], C. R. Boddy[119], M. Boehler[48], J. Boek[176], T. T. Boek[176], J. A. Bogaerts[30], A. G. Bogdanchikov[108], A. Bogouch[91,*], C. Bohm[147a], J. Bohm[126], V. Boisvert[76], T. Bold[38a], V. Boldea[26a], A. S. Boldyrev[98], M. Bomben[79], M. Bona[75], M. Boonekamp[137], A. Borisov[129], G. Borissov[71], M. Borri[83], S. Borroni[42], J. Bortfeldt[99], V. Bortolotto[135a,135b], K. Bos[106], D. Boscherini[20a], M. Bosman[12], H. Boterenbrood[106], J. Boudreau[124], J. Bouffard[2], E. V. Bouhova-Thacker[71], D. Boumediene[34], C. Bourdarios[116], N. Bousson[113], S. Boutouil[136d], A. Boveia[31], J. Boyd[30], I. R. Boyko[64], I. Bozovic-Jelisavcic[13b], J. Bracinik[18], P. Branchini[135a], A. Brandt[8], G. Brandt[15], O. Brandt[58a], U. Bratzler[157], B. Brau[85], J. E. Brau[115], H. M. Braun[176,*], S. F. Brazzale[165a,165c], B. Brelier[159], K. Brendlinger[121], A. J. Brennan[87], R. Brenner[167], S. Bressler[173], K. Bristow[146c], T. M. Bristow[46], D. Britton[53], F. M. Brochu[28], I. Brock[21], R. Brock[89], C. Bromberg[89], J. Bronner[100], G. Brooijmans[35], T. Brooks[76], W. K. Brooks[32b], J. Brosamer[15], E. Brost[115], G. Brown[83], J. Brown[55], P. A. Bruckman de Renstrom[39], D. Bruncko[145b], R. Bruneliere[48], S. Brunet[60], A. Bruni[20a], G. Bruni[20a], M. Bruschi[20a], L. Bryngemark[80], T. Buanes[14], Q. Buat[143], F. Bucci[49], P. Buchholz[142], R. M. Buckingham[119], A. G. Buckley[53], S. I. Buda[26a], I. A. Budagov[64], F. Buehrer[48], L. Bugge[118], M. K. Bugge[118], O. Bulekov[97], A. C. Bundock[73], H. Burckhart[30], S. Burdin[73], B. Burghgrave[107], S. Burke[130], I. Burmeister[43], E. Busato[34], D. Büscher[48], V. Büscher[82], P. Bussey[53], C. P. Buszello[167], B. Butler[57], J. M. Butler[22], A. I. Butt[3], C. M. Buttar[53], J. M. Butterworth[77], P. Butti[106], W. Buttinger[28], A. Buzatu[53], M. Byszewski[10], S. Cabrera Urbán[168], D. Caforio[20a,20b], O. Cakir[4a], P. Calafiura[15], A. Calandri[137], G. Calderini[79], P. Calfayan[99], R. Calkins[107], L. P. Caloba[24a], D. Calvet[34], S. Calvet[34], R. Camacho Toro[49], S. Camarda[42], D. Cameron[118], L. M. Caminada[15], R. Caminal Armadans[12], S. Campana[30], M. Campanelli[77], A. Campoverde[149], V. Canale[103a,103b], A. Canepa[160a], J. Cantero[81], R. Cantrill[76], T. Cao[40], M. D. M. Capeans Garrido[30], I. Caprini[26a], M. Caprini[26a], M. Capua[37a,37b], R. Caputo[82], R. Cardarelli[134a], T. Carli[30], G. Carlino[103a], L. Carminati[90a,90b], S. Caron[105], E. Carquin[32a], G. D. Carrillo-Montoya[146c], J. R. Carter[28], J. Carvalho[125a,125c], D. Casadei[77], M. P. Casado[12], M. Casolino[12], E. Castaneda-Miranda[146b], A. Castelli[106], V. Castillo Gimenez[168], N. F. Castro[125a], P. Catastini[57], A. Catinaccio[30], J. R. Catmore[118], A. Cattai[30], G. Cattani[134a,134b], S. Caughron[89], V. Cavaliere[166], D. Cavalli[90a], M. Cavalli-Sforza[12], V. Cavasinni[123a,123c], F. Ceradini[135a,135b], B. Cerio[45], K. Cerny[128], A. S. Cerqueira[24b], A. Cerri[150], L. Cerrito[75], F. Cerutti[15], M. Cerv[30], A. Cervelli[17], S. A. Cetin[19b], A. Chafaq[136a], D. Chakraborty[107], I. Chalupkova[128], K. Chan[3], P. Chang[166], B. Chapleau[86], J. D. Chapman[28], D. Charfeddine[116], D. G. Charlton[18], C. C. Chau[159], C. A. Chavez Barajas[150], S. Cheatham[86], A. Chegwidden[89], S. Chekanov[6], S. V. Chekulaev[160a], G. A. Chelkov[64], M. A. Chelstowska[88], C. Chen[63], H. Chen[25], K. Chen[149], L. Chen[33d,f], S. Chen[33c], X. Chen[146c], Y. Chen[35], H. C. Cheng[88], Y. Cheng[31], A. Cheplakov[64], R. Cherkaoui El Moursli[136e], V. Chernyatin[25,*], E. Cheu[7], L. Chevalier[137], V. Chiarella[47], G. Chiefari[103a,103b], J. T. Childers[6], A. Chilingarov[71], G. Chiodini[72a], A. S. Chisholm[18], R. T. Chislett[77], A. Chitan[26a], M. V. Chizhov[64], S. Chouridou[9], B. K. B. Chow[99], I. A. Christidi[77], D. Chromek-Burckhart[30], M. L. Chu[152], J. Chudoba[126], J. J. Chwastowski[39], L. Chytka[114], G. Ciapetti[133a,133b], A. K. Ciftci[4a], R. Ciftci[4a], D. Cinca[62], V. Cindro[74], A. Ciocio[15], P. Cirkovic[13b], Z. H. Citron[173], M. Citterio[90a], M. Ciubancan[26a], A. Clark[49], P. J. Clark[46], R. N. Clarke[15], W. Cleland[124], J. C. Clemens[84], C. Clement[147a,147b], Y. Coadou[84], M. Cobal[165a,165c], A. Coccaro[139], J. Cochran[63], L. Coffey[23], J. G. Cogan[144], J. Coggeshall[166], B. Cole[35], S. Cole[107], A. P. Colijn[106], C. Collins-Tooth[53], J. Collot[55], T. Colombo[58c], G. Colon[85], G. Compostella[100], P. Conde Muiño[125a,125b], E. Coniavitis[167], M. C. Conidi[12], S. H. Connell[146b], I. A. Connelly[76], S. M. Consonni[90a,90b], V. Consorti[48], S. Constantinescu[26a], C. Conta[120a,120b], G. Conti[57], F. Conventi[103a,g], M. Cooke[15], B. D. Cooper[77], A. M. Cooper-Sarkar[119], N. J. Cooper-Smith[76], K. Copic[15], T. Cornelissen[176], M. Corradi[20a], F. Corriveau[86,h], A. Corso-Radu[164], A. Cortes-Gonzalez[12], G. Cortiana[100], G. Costa[90a], M. J. Costa[168], D. Costanzo[140], D. Côté[8], G. Cottin[28], G. Cowan[76], B. E. Cox[83], K. Cranmer[109], G. Cree[29], S. Crépé-Renaudin[55], F. Crescioli[79], M. Crispin Ortuzar[119], M. Cristinziani[21], V. Croft[105], G. Crosetti[37a,37b], C.-M. Cuciuc[26a], T. Cuhadar Donszelmann[140], J. Cummings[177], M. Curatolo[47], C. Cuthbert[151], H. Czirr[142], P. Czodrowski[3], Z. Czyczula[177], S. D'Auria[53], M. D'Onofrio[73], M. J. Da Cunha Sargedas De Sousa[125a,125b], C. Da Via[83], W. Dabrowski[38a], A. Dafinca[119], T. Dai[88], O. Dale[14], F. Dallaire[94],

C. Dallapiccola[85], M. Dam[36], A. C. Daniells[18], M. Dano Hoffmann[137], V. Dao[105], G. Darbo[50a], G. L. Darlea[26c], S. Darmora[8], J. A. Dassoulas[42], A. Dattagupta[60], W. Davey[21], C. David[170], T. Davidek[128], E. Davies[119,c], M. Davies[154], O. Davignon[79], A. R. Davison[77], P. Davison[77], Y. Davygora[58a], E. Dawe[143], I. Dawson[140], R. K. Daya-Ishmukhametova[23], K. De[8], R. de Asmundis[103a], S. De Castro[20a,20b], S. De Cecco[79], J. de Graat[99], N. De Groot[105], P. de Jong[106], H. De la Torre[81], F. De Lorenzi[63], L. De Nooij[106], D. De Pedis[133a], A. De Salvo[133a], U. De Sanctis[165a,165b], A. De Santo[150], J. B. De Vivie De Regie[116], G. De Zorzi[133a,133b], W. J. Dearnaley[71], R. Debbe[25], C. Debenedetti[46], B. Dechenaux[55], D. V. Dedovich[64], J. Degenhardt[121], I. Deigaard[106], J. Del Peso[81], T. Del Prete[123a,123b], F. Deliot[137], C. M. Delitzsch[49], M. Deliyergiyev[74], A. Dell'Acqua[30], L. Dell'Asta[22], M. Dell'Orso[123a,123b], M. Della Pietra[103a,g], d. della Volpe[49], M. Delmastro[5], P. A. Delsart[55], C. Deluca[106], S. Demers[177], M. Demichev[64], A. Demilly[79], S. P. Denisov[129], D. Derendarz[39], J. E. Derkaoui[136d], F. Derue[79], P. Dervan[73], K. Desch[21], C. Deterre[42], P. O. Deviveiros[106], A. Dewhurst[130], S. Dhaliwal[106], A. Di Ciaccio[134a,134b], L. Di Ciaccio[5], A. Di Domenico[133a,133b], C. Di Donato[103a,103b], A. Di Girolamo[30], B. Di Girolamo[30], A. Di Mattia[153], B. Di Micco[135a,135b], R. Di Nardo[47], A. Di Simone[48], R. Di Sipio[20a,20b], D. Di Valentino[29], M. A. Diaz[32a], E. B. Diehl[88], J. Dietrich[42], T. A. Dietzsch[58a], S. Diglio[84], A. Dimitrievska[13a], J. Dingfelder[21], C. Dionisi[133a,133b], P. Dita[26a], S. Dita[26a], F. Dittus[30], F. Djama[84], T. Djobava[51b], M. A. B. do Vale[24c], A. Do Valle Wemans[125a,125g], T. K. O. Doan[5], D. Dobos[30], E. Dobson[77], C. Doglioni[49], T. Doherty[53], T. Dohmae[156], J. Dolejsi[128], Z. Dolezal[128], B. A. Dolgoshein[97,*], M. Donadelli[24d], S. Donati[123a,123b], P. Dondero[120a,120b], J. Donini[34], J. Dopke[30], A. Doria[103a], M. T. Dova[70], A. T. Doyle[53], M. Dris[10], J. Dubbert[88], S. Dube[15], E. Dubreuil[34], E. Duchovni[173], G. Duckeck[99], O. A. Ducu[26a], D. Duda[176], A. Dudarev[30], F. Dudziak[63], L. Duflot[116], L. Duguid[76], M. Dührssen[30], M. Dunford[58a], H. Duran Yildiz[4a], M. Düren[52], A. Durglishvili[51b], M. Dwuznik[38a], M. Dyndal[38a], J. Ebke[99], W. Edson[2], N. C. Edwards[46], W. Ehrenfeld[21], T. Eifert[144], G. Eigen[14], K. Einsweiler[15], T. Ekelof[167], M. El Kacimi[136c], M. Ellert[167], S. Elles[5], F. Ellinghaus[82], N. Ellis[30], J. Elmsheuser[99], M. Elsing[30], D. Emeliyanov[130], Y. Enari[156], O. C. Endner[82], M. Endo[117], R. Engelmann[149], J. Erdmann[177], A. Ereditato[17], D. Eriksson[147a], G. Ernis[176], J. Ernst[2], M. Ernst[25], J. Ernwein[137], D. Errede[166], S. Errede[166], E. Ertel[82], M. Escalier[116], H. Esch[43], C. Escobar[124], B. Esposito[47], A. I. Etienvre[137], E. Etzion[154], H. Evans[60], L. Fabbri[20a,20b], G. Facini[30], R. M. Fakhrutdinov[129], S. Falciano[133a], J. Faltova[128], Y. Fang[33a], M. Fanti[90a,90b], A. Farbin[8], A. Farilla[135a], T. Farooque[12], S. Farrell[164], S. M. Farrington[171], P. Farthouat[30], F. Fassi[168], P. Fassnacht[30], D. Fassouliotis[9], A. Favareto[50a,50b], L. Fayard[116], P. Federic[145a], O. L. Fedin[122,i], W. Fedorko[169], M. Fehling-Kaschek[48], S. Feigl[30], L. Feligioni[84], C. Feng[33d], E. J. Feng[6], H. Feng[88], A. B. Fenyuk[129], S. Fernandez Perez[30], S. Ferrag[53], J. Ferrando[53], A. Ferrari[167], P. Ferrari[106], R. Ferrari[120a], D. E. Ferreira de Lima[53], A. Ferrer[168], D. Ferrere[49], C. Ferretti[88], A. Ferretto Parodi[50a,50b], M. Fiascaris[31], F. Fiedler[82], A. Filipčič[74], M. Filipuzzi[42], F. Filthaut[105], M. Fincke-Keeler[170], K. D. Finelli[151], M. C. N. Fiolhais[125a,125c], L. Fiorini[168], A. Firan[40], J. Fischer[176], W. C. Fisher[89], E. A. Fitzgerald[23], M. Flechl[48], I. Fleck[142], P. Fleischmann[175], S. Fleischmann[176], G. T. Fletcher[140], G. Fletcher[75], T. Flick[176], A. Floderus[80], L. R. Flores Castillo[174], A. C. Florez Bustos[160b], M. J. Flowerdew[100], A. Formica[137], A. Forti[83], D. Fortin[160a], D. Fournier[116], H. Fox[71], S. Fracchia[12], P. Francavilla[79], M. Franchini[20a,20b], S. Franchino[30], D. Francis[30], M. Franklin[57], S. Franz[61], M. Fraternali[120a,120b], S. T. French[28], C. Friedrich[42], F. Friedrich[44], D. Froidevaux[30], J. A. Frost[28], C. Fukunaga[157], E. Fullana Torregrosa[82], B. G. Fulsom[144], J. Fuster[168], C. Gabaldon[55], O. Gabizon[173], A. Gabrielli[20a,20b], A. Gabrielli[133a,133b], S. Gadatsch[106], S. Gadomski[49], G. Gagliardi[50a,50b], P. Gagnon[60], C. Galea[105], B. Galhardo[125a,125c], E. J. Gallas[119], V. Gallo[17], B. J. Gallop[130], P. Gallus[127], G. Galster[36], K. K. Gan[110], R. P. Gandrajula[62], J. Gao[33b,f], Y. S. Gao[144,e], F. M. Garay Walls[46], F. Garberson[177], C. García[168], J. E. García Navarro[168], M. Garcia-Sciveres[15], R. W. Gardner[31], N. Garelli[144], V. Garonne[30], C. Gatti[47], G. Gaudio[120a], B. Gaur[142], L. Gauthier[94], P. Gauzzi[133a,133b], I. L. Gavrilenko[95], C. Gay[169], G. Gaycken[21], E. N. Gazis[10], P. Ge[33d], Z. Gecse[169], C. N. P. Gee[130], D. A. A. Geerts[106], Ch. Geich-Gimbel[21], K. Gellerstedt[147a,147b], C. Gemme[50a], A. Gemmell[53], M. H. Genest[55], S. Gentile[133a,133b], M. George[54], S. George[76], D. Gerbaudo[164], A. Gershon[154], H. Ghazlane[136b], N. Ghodbane[34], B. Giacobbe[20a], S. Giagu[133a,133b], V. Giangiobbe[12], P. Giannetti[123a,123b], F. Gianotti[30], B. Gibbard[25], S. M. Gibson[76], M. Gilchriese[15], T. P. S. Gillam[28], D. Gillberg[30], G. Gilles[34], D. M. Gingrich[3,d], N. Giokaris[9], M. P. Giordani[165a,165c], R. Giordano[103a,103b], F. M. Giorgi[16], P. F. Giraud[137], D. Giugni[90a], C. Giuliani[48], M. Giulini[58b], B. K. Gjelsten[118], I. Gkialas[155,j], L. K. Gladilin[98], C. Glasman[81], J. Glatzer[30], P. C. F. Glaysher[46], A. Glazov[42], G. L. Glonti[64], M. Goblirsch-Kolb[100], J. R. Goddard[75], J. Godfrey[143], J. Godlewski[30], C. Goeringer[82], S. Goldfarb[88], T. Golling[177], D. Golubkov[129], A. Gomes[125a,125b,125d], L. S. Gomez Fajardo[42], R. Gonçalo[125a], J. Goncalves Pinto Firmino Da Costa[42], L. Gonella[21], S. González de la Hoz[168], G. Gonzalez Parra[12], M. L. Gonzalez Silva[27], S. Gonzalez-Sevilla[49], L. Goossens[30], P. A. Gorbounov[96], H. A. Gordon[25], I. Gorelov[104], B. Gorini[30], E. Gorini[72a,72b], A. Gorišek[74], E. Gornicki[39], A. T. Goshaw[6], C. Gössling[43], M. I. Gostkin[64], M. Gouighri[136a], D. Goujdami[136c], M. P. Goulette[49], A. G. Goussiou[139], C. Goy[5], S. Gozpinar[23], H. M. X. Grabas[137], L. Graber[54], I. Grabowska-Bold[38a], P. Grafström[20a,20b], K-J. Grahn[42], J. Gramling[49], E. Gramstad[118], S. Grancagnolo[16], V. Grassi[149], V. Gratchev[122], H. M. Gray[30], E. Graziani[135a], O. G. Grebenyuk[122], Z. D. Greenwood[78,k], K. Gregersen[77], I. M. Gregor[42], P. Grenier[144], J. Griffiths[8], A. A. Grillo[138], K. Grimm[71], S. Grinstein[12,l], Ph. Gris[34], Y. V. Grishkevich[98], J-F. Grivaz[116], J. P. Grohs[44], A. Grohsjean[42], E. Gross[173], J. Grosse-Knetter[54], G. C. Grossi[134a,134b], J.

Groth-Jensen[173], Z. J. Grout[150], K. Grybel[142], L. Guan[33b], F. Guescini[49], D. Guest[177], O. Gueta[154], C. Guicheney[34], E. Guido[50a,50b], T. Guillemin[116], S. Guindon[2], U. Gul[53], C. Gumpert[44], J. Gunther[127], J. Guo[35], S. Gupta[119], P. Gutierrez[112], N. G. Gutierrez Ortiz[53], C. Gutschow[77], N. Guttman[154], C. Guyot[137], C. Gwenlan[119], C. B. Gwilliam[73], A. Haas[109], C. Haber[15], H. K. Hadavand[8], N. Haddad[136e], P. Haefner[21], S. Hageboeck[21], Z. Hajduk[39], H. Hakobyan[178], M. Haleem[42], D. Hall[119], G. Halladjian[89], K. Hamacher[176], P. Hamal[114], K. Hamano[87], M. Hamer[54], A. Hamilton[146a], S. Hamilton[162], P. G. Hamnett[42], L. Han[33b], K. Hanagaki[117], K. Hanawa[156], M. Hance[15], P. Hanke[58a], J. B. Hansen[36], J. D. Hansen[36], P. H. Hansen[36], K. Hara[161], A. S. Hard[174], T. Harenberg[176], S. Harkusha[91], D. Harper[88], R. D. Harrington[46], O. M. Harris[139], P. F. Harrison[171], F. Hartjes[106], S. Hasegawa[102], Y. Hasegawa[141], A. Hasib [112], S. Hassani[137], S. Haug[17], M. Hauschild[30], R. Hauser[89], M. Havranek[126], C. M. Hawkes[18], R. J. Hawkings[30], A. D. Hawkins[80], T. Hayashi[161], D. Hayden[89], C. P. Hays[119], H. S. Hayward[73], S. J. Haywood[130], S. J. Head[18], T. Heck[82], V. Hedberg[80], L. Heelan[8], S. Heim[121], T. Heim[176], B. Heinemann[15], L. Heinrich[109], S. Heisterkamp[36], J. Hejbal[126], L. Helary[22], C. Heller[99], M. Heller[30], S. Hellman[147a,147b], D. Hellmich[21], C. Helsens[30], J. Henderson[119], R. C. W. Henderson[71], C. Hengler[42], A. Henrichs[177], A. M. Henriques Correia[30], S. Henrot-Versille[116], C. Hensel[54], G. H. Herbert[16], Y. Hernández Jiménez[168], R. Herrberg-Schubert[16], G. Herten[48], R. Hertenberger[99], L. Hervas[30], G. G. Hesketh[77], N. P. Hessey[106], R. Hickling[75], E. Higón-Rodriguez[168], E. Hill[170], J. C. Hill[28], K. H. Hiller[42], S. Hillert[21], S. J. Hillier[18], I. Hinchliffe[15], E. Hines[121], M. Hirose[117], D. Hirschbuehl[176], J. Hobbs[149], N. Hod[106], M. C. Hodgkinson[140], P. Hodgson[140], A. Hoecker[30], M. R. Hoeferkamp[104], J. Hoffman[40], D. Hoffmann[84], J. I. Hofmann[58a], M. Hohlfeld[82], T. R. Holmes[15], T. M. Hong[121], L. Hooft van Huysduynen[109], J-Y. Hostachy[55], S. Hou[152], A. Hoummada[136a], J. Howard[119], J. Howarth[42], M. Hrabovsky[114], I. Hristova[16], J. Hrivnac[116], T. Hryn'ova[5], P. J. Hsu[82], S.-C. Hsu[139], D. Hu[35], X. Hu[25], Y. Huang[42], Z. Hubacek[30], F. Hubaut[84], F. Huegging[21], T. B. Huffman[119], E. W. Hughes[35], G. Hughes[71], M. Huhtinen[30], T. A. Hülsing[82], M. Hurwitz[15], N. Huseynov[64,b], J. Huston[89], J. Huth[57], G. Iacobucci[49], G. Iakovidis[10], I. Ibragimov[142], L. Iconomidou-Fayard[116], E. Ideal[177], P. Iengo[103a], O. Igonkina[106], T. Iizawa[172], Y. Ikegami[65], K. Ikematsu[142], M. Ikeno[65], D. Iliadis[155], N. Ilic[159], Y. Inamaru[66], T. Ince[100], P. Ioannou[9], M. Iodice[135a], K. Iordanidou[9], V. Ippolito[57], A. Irles Quiles[168], C. Isaksson[167], M. Ishino[67], M. Ishitsuka[158], R. Ishmukhametov[110], C. Issever[119], S. Istin[19a], J. M. Iturbe Ponce[83], J. Ivarsson[80], A. V. Ivashin[129], W. Iwanski[39], H. Iwasaki[65], J. M. Izen[41], V. Izzo[103a], B. Jackson[121], M. Jackson[73], P. Jackson[1], M. R. Jaekel[30], V. Jain[2], K. Jakobs[48], S. Jakobsen[30], T. Jakoubek[126], J. Jakubek[127], D. O. Jamin[152], D. K. Jana[78], E. Jansen[77], H. Jansen[30], J. Janssen[21], M. Janus[171], G. Jarlskog[80], N. Javadov[64,b], T. Javůrek[48], L. Jeanty[15], G.-Y. Jeng[151], D. Jennens[87], P. Jenni[48,m], J. Jentzsch[43], C. Jeske[171], S. Jézéquel[5], H. Ji[174], W. Ji[82], J. Jia[149], Y. Jiang[33b], M. Jimenez Belenguer[42], S. Jin[33a], A. Jinaru[26a], O. Jinnouchi[158], M. D. Joergensen[36], K. E. Johansson[147a], P. Johansson[140], K. A. Johns[7], K. Jon-And[147a,147b], G. Jones[171], R. W. L. Jones[71], T. J. Jones[73], J. Jongmanns[58a], P. M. Jorge[125a,125b], K. D. Joshi[83], J. Jovicevic[148], X. Ju[174], C. A. Jung[43], R. M. Jungst[30], P. Jussel[61], A. Juste Rozas[12,l], M. Kaci[168], A. Kaczmarska[39], M. Kado[116], H. Kagan[110], M. Kagan[144], E. Kajomovitz[45], S. Kama[40], N. Kanaya[156], M. Kaneda[30], S. Kaneti[28], T. Kanno[158], V. A. Kantserov[97], J. Kanzaki[65], B. Kaplan[109], A. Kapliy[31], D. Kar[53], K. Karakostas[10], N. Karastathis[10], M. Karnevskiy[82], S. N. Karpov[64], Z. M. Karpova[64], K. Karthik[109], V. Kartvelishvili[71], A. N. Karyukhin[129], L. Kashif[174], G. Kasieczka[58b], R. D. Kass[110], A. Kastanas[14], Y. Kataoka[156], A. Katre[49], J. Katzy[42], V. Kaushik[7], K. Kawagoe[69], T. Kawamoto[156], G. Kawamura[54], S. Kazama[156], V. F. Kazanin[108], M. Y. Kazarinov[64], R. Keeler[170], R. Kehoe[40], M. Keil[54], J. S. Keller[42], H. Keoshkerian[5], O. Kepka[126], B. P. Kerševan[74], S. Kersten[176], K. Kessoku[156], J. Keung[159], F. Khalil-zada[11], H. Khandanyan[147a,147b], A. Khanov[113], A. Khodinov[97], A. Khomich[58a], T. J. Khoo[28], G. Khoriauli[21], A. Khoroshilov[176], V. Khovanskiy[96], E. Khramov[64], J. Khubua[51b], H. Y. Kim[8], H. Kim[147a,147b], S. H. Kim[161], N. Kimura[172], O. Kind[16], B. T. King[73], M. King[168], R. S. B. King[119], S. B. King[169], J. Kirk[130], A. E. Kiryunin[100], T. Kishimoto[66], D. Kisielewska[38a], F. Kiss[48], T. Kitamura[66], T. Kittelmann[124], K. Kiuchi[161], E. Kladiva[145b], M. Klein[73], U. Klein[73], K. Kleinknecht[82], P. Klimek[147a,147b], A. Klimentov[25], R. Klingenberg[43], J. A. Klinger[83], T. Klioutchnikova[30], P. F. Klok[105], E.-E. Kluge[58a], P. Kluit[106], S. Kluth[100], E. Kneringer[61], E. B. F. G. Knoops[84], A. Knue[53], T. Kobayashi[156], M. Kobel[44], M. Kocian[144], P. Kodys[128], P. Koevesarki[21], T. Koffas[29], E. Koffeman[106], L. A. Kogan[119], S. Kohlmann[176], Z. Kohout[127], T. Kohriki[65], T. Koi[144], H. Kolanoski[16], I. Koletsou[5], J. Koll[89], A. A. Komar[95,*], Y. Komori[156], T. Kondo[65], N. Kondrashova[42], K. Köneke[48], A. C. König[105], S. König[82], T. Kono[65,n], R. Konoplich[109,o], N. Konstantinidis[77], R. Kopeliansky[153], S. Koperny[38a], L. Köpke[82], A. K. Kopp[48], K. Korcyl[39], K. Kordas[155], A. Korn[77], A. A. Korol[108,p], I. Korolkov[12], E. V. Korolkova[140], V. A. Korotkov[129], O. Kortner[100], S. Kortner[100], V. V. Kostyukhin[21], V. M. Kotov[64], A. Kotwal[45], C. Kourkoumelis[9], V. Kouskoura[155], A. Koutsman[160a], R. Kowalewski[170], T. Z. Kowalski[38a], W. Kozanecki[137], A. S. Kozhin[129], V. Kral[127], V. A. Kramarenko[98], G. Kramberger[74], D. Krasnopevtsev[97], M. W. Krasny[79], A. Krasznahorkay[30], J. K. Kraus[21], A. Kravchenko[25], S. Kreiss[109], M. Kretz[58c], J. Kretzschmar[73], K. Kreutzfeldt[52], P. Krieger[159], K. Kroeninger[54], H. Kroha[100], J. Kroll[121], J. Kroseberg[21], J. Krstic[13a], U. Kruchonak[64], H. Krüger[21], T. Kruker[17], N. Krumnack[63], Z. V. Krumshteyn[64], A. Kruse[174], M. C. Kruse[45], M. Kruskal[22], T. Kubota[87], S. Kuday[4a], S. Kuehn[48], A. Kugel[58c], A. Kuhl[138], T. Kuhl[42], V. Kukhtin[64], Y. Kulchitsky[91], S. Kuleshov[32b], M. Kuna[133a,133b], J. Kunkle[121], A. Kupco[126], H. Kurashige[66], Y. A. Kurochkin[91], R. Kurumida[66], V. Kus[126], E. S. Kuwertz[148],

M. Kuze[158], J. Kvita[114], A. La Rosa[49], L. La Rotonda[37a,37b], C. Lacasta[168], F. Lacava[133a,133b], J. Lacey[29], H. Lacker[16], D. Lacour[79], V. R. Lacuesta[168], E. Ladygin[64], R. Lafaye[5], B. Laforge[79], T. Lagouri[177], S. Lai[48], H. Laier[58a], L. Lambourne[77], S. Lammers[60], C. L. Lampen[7], W. Lampl[7], E. Lançon[137], U. Landgraf[48], M. P. J. Landon[75], V. S. Lang[58a], C. Lange[42], A. J. Lankford[164], F. Lanni[25], K. Lantzsch[30], S. Laplace[79], C. Lapoire[21], J. F. Laporte[137], T. Lari[90a], M. Lassnig[30], P. Laurelli[47], W. Lavrijsen[15], A. T. Law[138], P. Laycock[73], B. T. Le[55], O. Le Dortz[79], E. Le Guirriec[84], E. Le Menedeu[12], T. LeCompte[6], F. Ledroit-Guillon[55], C. A. Lee[152], H. Lee[106], J. S. H. Lee[117], S. C. Lee[152], L. Lee[177], G. Lefebvre[79], M. Lefebvre[170], F. Legger[99], C. Leggett[15], A. Lehan[73], M. Lehmacher[21], G. Lehmann Miotto[30], X. Lei[7], A. G. Leister[177], M. A. L. Leite[24d], R. Leitner[128], D. Lellouch[173], B. Lemmer[54], K. J. C. Leney[77], T. Lenz[106], G. Lenzen[176], B. Lenzi[30], R. Leone[7], K. Leonhardt[44], S. Leontsinis[10], C. Leroy[94], C. G. Lester[28], C. M. Lester[121], M. Levchenko[122], J. Levêque[5], D. Levin[88], L. J. Levinson[173], M. Levy[18], A. Lewis[119], G. H. Lewis[109], A. M. Leyko[21], M. Leyton[41], B. Li[33b,q], B. Li[84], H. Li[149], H. L. Li[31], L. Li[33e], S. Li[45], Y. Li[33c,r], Z. Liang[119,s], H. Liao[34], B. Liberti[134a], P. Lichard[30], K. Lie[166], J. Liebal[21], W. Liebig[14], C. Limbach[21], A. Limosani[87], M. Limper[62], S. C. Lin[152,t], F. Linde[106], B. E. Lindquist[149], J. T. Linnemann[89], E. Lipeles[121], A. Lipniacka[14], M. Lisovyi[42], T. M. Liss[166], D. Lissauer[25], A. Lister[169], A. M. Litke[138], B. Liu[152], D. Liu[152], J. B. Liu[33b], K. Liu[33b,u], L. Liu[88], M. Liu[45], M. Liu[33b], Y. Liu[33b], M. Livan[120a,120b], S. S. A. Livermore[119], A. Lleres[55], J. Llorente Merino[81], S. L. Lloyd[75], F. Lo Sterzo[152], E. Lobodzinska[42], P. Loch[7], W. S. Lockman[138], T. Loddenkoetter[21], F. K. Loebinger[83], A. E. Loevschall-Jensen[36], A. Loginov[177], C. W. Loh[169], T. Lohse[16], K. Lohwasser[48], M. Lokajicek[126], V. P. Lombardo[5], B. A. Long[22], J. D.Long[88], R. E. Long[71], L. Lopes[125a], D. Lopez Mateos[57], B. Lopez Paredes[140], J. Lorenz[99], N. Lorenzo Martinez[60], M. Losada[163], P. Loscutoff[15], X. Lou[41], A. Lounis[116], J. Love[6], P. A. Love[71], A. J. Lowe[144,e], F. Lu[33a], H. J. Lubatti[139], C. Luci[133a,133b], A. Lucotte[55], F. Luehring[60], W. Lukas[61], L. Luminari[133a], O. Lundberg[147a,147b], B. Lund-Jensen[148], M. Lungwitz[82], D. Lynn[25], R. Lysak[126], E. Lytken[80], H. Ma[25], L. L. Ma[33d], G. Maccarrone[47], A. Macchiolo[100], J. Machado Miguens[125a,125b], D. Macina[30], D. Madaffari[84], R. Madar[48], H. J. Maddocks[71], W. F. Mader[44], A. Madsen[167], M. Maeno[8], T. Maeno[25], E. Magradze[54], K. Mahboubi[48], J. Mahlstedt[106], S. Mahmoud[73], C. Maiani[137], C. Maidantchik[24a], A. Maio[125a,125b,125d], S. Majewski[115], Y. Makida[65], N. Makovec[116], P. Mal[137,v], B. Malaescu[79], Pa. Malecki[39], V. P. Maleev[122], F. Malek[55], U. Mallik[62], D. Malon[6], C. Malone[144], S. Maltezos[10], V. M. Malyshev[108], S. Malyukov[30], J. Mamuzic[13b], B. Mandelli[30], L. Mandelli[90a], I. Mandić[74], R. Mandrysch[62], J. Maneira[125a,125b], A. Manfredini[100], L. Manhaes de Andrade Filho[24b], J. A. Manjarres Ramos[160b], A. Mann[99], P. M. Manning[138], A. Manousakis-Katsikakis[9], B. Mansoulie[137], R. Mantifel[86], L. Mapelli[30], L. March[168], J. F. Marchand[29], G. Marchiori[79], M. Marcisovsky[126], C. P. Marino[170], C. N. Marques[125a], F. Marroquim[24a], S. P. Marsden[83], Z. Marshall[15], L. F. Marti[17], S. Marti-Garcia[168], B. Martin[30], B. Martin[89], T. A. Martin[171], V. J. Martin[46], B. Martin dit Latour[14], H. Martinez[137], M. Martinez[12,l], S. Martin-Haugh[130], A. C. Martyniuk[77], M. Marx[139], F. Marzano[133a], A. Marzin[30], L. Masetti[82], T. Mashimo[156], R. Mashinistov[95], J. Masik[83], A. L. Maslennikov[108], I. Massa[20a,20b], N. Massol[5], P. Mastrandrea[149], A. Mastroberardino[37a,37b], T. Masubuchi[156], H. Matsunaga[156], T. Matsushita[66], P. Mättig[176], S. Mättig[42], J. Mattmann[82], J. Maurer[26a], S. J. Maxfield[73], D. A. Maximov[108,p], R. Mazini[152], L. Mazzaferro[134a,134b], G. Mc Goldrick[159], S. P. Mc Kee[88], A. McCarn[88], R. L. McCarthy[149], T. G. McCarthy[29], N. A. McCubbin[130], K. W. McFarlane[56,*], J. A. Mcfayden[77], G. Mchedlidze[54], T. Mclaughlan[18], S. J. McMahon[130], R. A. McPherson[170,h], A. Meade[85], J. Mechnich[106], M. Medinnis[42], S. Meehan[31], S. Mehlhase[36], A. Mehta[73], K. Meier[58a], C. Meineck[99], B. Meirose[80], C. Melachrinos[31], B. R. Mellado Garcia[146c], F. Meloni[90a,90b], A. Mengarelli[20a,20b], S. Menke[100], E. Meoni[162], K. M. Mercurio[57], S. Mergelmeyer[21], N. Meric[137], P. Mermod[49], L. Merola[103a,103b], C. Meroni[90a], F. S. Merritt[31], H. Merritt[110], A. Messina[30,w], J. Metcalfe[25], A. S. Mete[164], C. Meyer[82], C. Meyer[31], J-P. Meyer[137], J. Meyer[30], R. P. Middleton[130], S. Migas[73], L. Mijović[137], G. Mikenberg[173], M. Mikestikova[126], M. Mikuž[74], D. W. Miller[31], C. Mills[46], A. Milov[173], D. A. Milstead[147a,147b], D. Milstein[173], A. A. Minaenko[129], I. A. Minashvili[64], A. I. Mincer[109], B. Mindur[38a], M. Mineev[64], Y. Ming[174], L. M. Mir[12], G. Mirabelli[133a], T. Mitani[172], J. Mitrevski[99], V. A. Mitsou[168], S. Mitsui[65], A. Miucci[49], P. S. Miyagawa[140], J. U. Mjörnmark[80], T. Moa[147a,147b], K. Mochizuki[84], V. Moeller[28], S. Mohapatra[35], W. Mohr[48], S. Molander[147a,147b], R. Moles-Valls[168], K. Mönig[42], C. Monini[55], J. Monk[36], E. Monnier[84], J. Montejo Berlingen[12], F. Monticelli[70], S. Monzani[133a,133b], R. W. Moore[3], A. Moraes[53], N. Morange[62], J. Morel[54], D. Moreno[82], M. Moreno Llácer[54], P. Morettini[50a], M. Morgenstern[44], M. Morii[57], S. Moritz[82], A. K. Morley[148], G. Mornacchi[30], J. D. Morris[75], L. Morvaj[102], H. G. Moser[100], M. Mosidze[51b], J. Moss[110], R. Mount[144], E. Mountricha[25], S. V. Mouraviev[95,*], E. J. W. Moyse[85], S. Muanza[84], R. D. Mudd[18], F. Mueller[58a], J. Mueller[124], K. Mueller[21], T. Mueller[28], T. Mueller[82], D. Muenstermann[49], Y. Munwes[154], J. A. Murillo Quijada[18], W. J. Murray[171,130], H. Musheghyan[54], E. Musto[153], A. G. Myagkov[129,x], M. Myska[127], O. Nackenhorst[54], J. Nadal[54], K. Nagai[61], R. Nagai[158], Y. Nagai[84], K. Nagano[65], A. Nagarkar[110], Y. Nagasaka[59], M. Nagel[100], A. M. Nairz[30], Y. Nakahama[30], K. Nakamura[65], T. Nakamura[156], I. Nakano[111], H. Namasivayam[41], G. Nanava[21], R. Narayan[58b], T. Nattermann[21], T. Naumann[42], G. Navarro[163], R. Nayyar[7], H. A. Neal[88], P. Yu. Nechaeva[95], T. J. Neep[83], A. Negri[120a,120b], G. Negri[30], M. Negrini[20a], S. Nektarijevic[49], A. Nelson[164], T. K. Nelson[144], S. Nemecek[126], P. Nemethy[109], A. A. Nepomuceno[24a], M. Nessi[30,y], M. S. Neubauer[166], M. Neumann[176], R. M. Neves[109], P. Nevski[25], P. R. Newman[18], D. H. Nguyen[6], R. B. Nickerson[119], R. Nicolaidou[137],

B. Nicquevert[30], J. Nielsen[138], N. Nikiforou[35], A. Nikiforov[16], V. Nikolaenko[129,x], I. Nikolic-Audit[79], K. Nikolics[49], K. Nikolopoulos[18], P. Nilsson[8], Y. Ninomiya[156], A. Nisati[133a], R. Nisius[100], T. Nobe[158], L. Nodulman[6], M. Nomachi[117], I. Nomidis[155], S. Norberg[112], M. Nordberg[30], S. Nowak[100], M. Nozaki[65], L. Nozka[114], K. Ntekas[10], G. Nunes Hanninger[87], T. Nunnemann[99], E. Nurse[77], F. Nuti[87], B. J. O'Brien[46], F. O'grady[7], D. C. O'Neil[143], V. O'Shea[53], F. G. Oakham[29,d], H. Oberlack[100], T. Obermann[21], J. Ocariz[79], A. Ochi[66], M. I. Ochoa[77], S. Oda[69], S. Odaka[65], H. Ogren[60], A. Oh[83], S. H. Oh[45], C. C. Ohm[30], H. Ohman[167], T. Ohshima[102], W. Okamura[117], H. Okawa[25], Y. Okumura[31], T. Okuyama[156], A. Olariu[26a], A. G. Olchevski[64], S. A. Olivares Pino[46], D. Oliveira Damazio[25], E. Oliver Garcia[168], A. Olszewski[39], J. Olszowska[39], A. Onofre[125a,125e], P. U. E. Onyisi[31,z], C. J. Oram[160a], M. J. Oreglia[31], Y. Oren[154], D. Orestano[135a,135b], N. Orlando[72a,72b], C. Oropeza Barrera[53], R. S. Orr[159], B. Osculati[50a,50b], R. Ospanov[121], G. Otero y Garzon[27], H. Otono[69], M. Ouchrif[136d], E. A. Ouellette[170], F. Ould-Saada[118], A. Ouraou[137], K. P. Oussoren[106], Q. Ouyang[33a], A. Ovcharova[15], M. Owen[83], V. E. Ozcan[19a], N. Ozturk[8], K. Pachal[119], A. Pacheco Pages[12], C. Padilla Aranda[12], M. Pagáčová[48], S. Pagan Griso[15], E. Paganis[140], C. Pahl[100], F. Paige[25], P. Pais[85], K. Pajchel[118], G. Palacino[160b], S. Palestini[30], D. Pallin[34], A. Palma[125a,125b], J. D. Palmer[18], Y. B. Pan[174], E. Panagiotopoulou[10], J. G. Panduro Vazquez[76], P. Pani[106], N. Panikashvili[88], S. Panitkin[25], D. Pantea[26a], L. Paolozzi[134a,134b], Th. D. Papadopoulou[10], K. Papageorgiou[155,j], A. Paramonov[6], D. Paredes Hernandez[34], M. A. Parker[28], F. Parodi[50a,50b], J. A. Parsons[35], U. Parzefall[48], E. Pasqualucci[133a], S. Passaggio[50a], A. Passeri[135a], F. Pastore[135a,135b,*], Fr. Pastore[76], G. Pásztor[49,aa], S. Pataraia[176], N. D. Patel[151], J. R. Pater[83], S. Patricelli[103a,103b], T. Pauly[30], J. Pearce[170], M. Pedersen[118], S. Pedraza Lopez[168], R. Pedro[125a,125b], S. V. Peleganchuk[108], D. Pelikan[167], H. Peng[33b], B. Penning[31], J. Penwell[60], D. V. Perepelitsa[25], E. Perez Codina[160a], M. T. Pérez García-Estañ[168], V. Perez Reale[35], L. Perini[90a,90b], H. Pernegger[30], R. Perrino[72a], R. Peschke[42], V. D. Peshekhonov[64], K. Peters[30], R. F. Y. Peters[83], B. A. Petersen[87], J. Petersen[30], T. C. Petersen[36], E. Petit[42], A. Petridis[147a,147b], C. Petridou[155], E. Petrolo[133a], F. Petrucci[135a,135b], M. Petteni[143], N. E. Pettersson[158], R. Pezoa[32b], P. W. Phillips[130], G. Piacquadio[144], E. Pianori[171], A. Picazio[49], E. Piccaro[75], M. Piccinini[20a,20b], R. Piegaia[27], D. T. Pignotti[110], J. E. Pilcher[31], A. D. Pilkington[77], J. Pina[125a,125b,125d], M. Pinamonti[165a,165c,ab], A. Pinder[119], J. L. Pinfold[3], A. Pingel[36], B. Pinto[125a], S. Pires[79], M. Pitt[173], C. Pizio[90a,90b], M.-A. Pleier[25], V. Pleskot[128], E. Plotnikova[64], P. Plucinski[147a,147b], S. Poddar[58a], F. Podlyski[34], R. Poettgen[82], L. Poggioli[116], D. Pohl[21], M. Pohl[49], G. Polesello[120a], A. Policicchio[37a,37b], R. Polifka[159], A. Polini[20a], C. S. Pollard[45], V. Polychronakos[25], K. Pommès[30], L. Pontecorvo[133a], B. G. Pope[89], G. A. Popeneciu[26b], D. S. Popovic[13a], A. Poppleton[30], X. Portell Bueso[12], G. E. Pospelov[100], S. Pospisil[127], K. Potamianos[15], I. N. Potrap[64], C. J. Potter[150], C. T. Potter[115], G. Poulard[30], J. Poveda[60], V. Pozdnyakov[64], P. Pralavorio[84], A. Pranko[15], S. Prasad[30], R. Pravahan[8], S. Prell[63], D. Price[83], J. Price[73], L. E. Price[6], D. Prieur[124], M. Primavera[72a], M. Proissl[46], K. Prokofiev[47], F. Prokoshin[32b], E. Protopapadaki[137], S. Protopopescu[25], J. Proudfoot[6], M. Przybycien[38a], H. Przysiezniak[5], E. Ptacek[115], E. Pueschel[85], D. Puldon[149], M. Purohit[25,ac], P. Puzo[116], J. Qian[88], G. Qin[53], Y. Qin[83], A. Quadt[54], D. R. Quarrie[15], W. B. Quayle[165a,165b], D. Quilty[53], A. Qureshi[160b], V. Radeka[25], V. Radescu[42], S. K. Radhakrishnan[149], P. Radloff[115], P. Rados[87], F. Ragusa[90a,90b], G. Rahal[179], S. Rajagopalan[25], M. Rammensee[30], A. S. Randle-Conde[40], C. Rangel-Smith[167], K. Rao[164], F. Rauscher[99], T. C. Rave[48], T. Ravenscroft[53], M. Raymond[30], A. L. Read[118], D. M. Rebuzzi[120a,120b], A. Redelbach[175], G. Redlinger[25], R. Reece[138], K. Reeves[41], L. Rehnisch[16], A. Reinsch[115], H. Reisin[27], M. Relich[164], C. Rembser[30], Z. L. Ren[152], A. Renaud[116], M. Rescigno[133a], S. Resconi[90a], O. L. Rezanova[108,p], P. Reznicek[128], R. Rezvani[94], R. Richter[100], M. Ridel[79], P. Rieck[16], M. Rijssenbeek[149], A. Rimoldi[120a,120b], L. Rinaldi[20a], E. Ritsch[61], I. Riu[12], F. Rizatdinova[113], E. Rizvi[75], S. H. Robertson[86,h], A. Robichaud-Veronneau[119], D. Robinson[28], J. E. M. Robinson[83], A. Robson[53], C. Roda[123a,123b], L. Rodrigues[30], S. Roe[30], O. Røhne[118], S. Rolli[162], A. Romaniouk[97], M. Romano[20a,20b], G. Romeo[27], E. Romero Adam[168], N. Rompotis[139], L. Roos[79], E. Ros[168], S. Rosati[133a], K. Rosbach[49], M. Rose[76], P. L. Rosendahl[14], O. Rosenthal[142], V. Rossetti[147a,147b], E. Rossi[103a,103b], L. P. Rossi[50a], R. Rosten[139], M. Rotaru[26a], I. Roth[173], J. Rothberg[139], D. Rousseau[116], C. R. Royon[137], A. Rozanov[84], Y. Rozen[153], X. Ruan[146c], F. Rubbo[12], I. Rubinskiy[42], V. I. Rud[98], C. Rudolph[44], M. S. Rudolph[159], F. Rühr[48], A. Ruiz-Martinez[30], Z. Rurikova[48], N. A. Rusakovich[64], A. Ruschke[99], J. P. Rutherfoord[7], N. Ruthmann[48], Y. F. Ryabov[122], M. Rybar[128], G. Rybkin[116], N. C. Ryder[119], A. F. Saavedra[151], S. Sacerdoti[27], A. Saddique[3], I. Sadeh[154], H. F-W. Sadrozinski[138], R. Sadykov[64], F. Safai Tehrani[133a], H. Sakamoto[156], Y. Sakurai[172], G. Salamanna[75], A. Salamon[134a], M. Saleem[112], D. Salek[106], P. H. Sales De Bruin[139], D. Salihagic[100], A. Salnikov[144], J. Salt[168], B. M. Salvachua Ferrando[6], D. Salvatore[37a,37b], F. Salvatore[150], A. Salvucci[105], A. Salzburger[30], D. Sampsonidis[155], A. Sanchez[103a,103b], J. Sánchez[168], V. Sanchez Martinez[168], H. Sandaker[14], R. L. Sandbach[75], H. G. Sander[82], M. P. Sanders[99], M. Sandhoff[176], T. Sandoval[28], C. Sandoval[163], R. Sandstroem[100], D. P. C. Sankey[130], A. Sansoni[47], C. Santoni[34], R. Santonico[134a,134b], H. Santos[125a], I. Santoyo Castillo[150], K. Sapp[124], A. Sapronov[64], J. G. Saraiva[125a,125d], B. Sarrazin[21], G. Sartisohn[176], O. Sasaki[65], Y. Sasaki[156], G. Sauvage[5,*], E. Sauvan[5], P. Savard[156,d], D. O. Savu[30], C. Sawyer[119], L. Sawyer[78,k], D. H. Saxon[53], J. Saxon[121], C. Sbarra[20a], A. Sbrizzi[3], T. Scanlon[30], D. A. Scannicchio[164], M. Scarcella[151], J. Schaarschmidt[173], P. Schacht[100], D. Schaefer[121], R. Schaefer[42], S. Schaepe[21], S. Schaetzel[58b], U. Schäfer[82], A. C. Schaffer[116], D. Schaile[99], R. D. Schamberger[149], V. Scharf[58a], V. A. Schegelsky[122], D. Scheirich[128], M. Schernau[164], M. I. Scherzer[35], C. Schiavi[50a,50b], J. Schieck[99], C. Schillo[48], M.

Schioppa[37a,37b], S. Schlenker[30], E. Schmidt[48], K. Schmieden[30], C. Schmitt[82], C. Schmitt[99], S. Schmitt[58b], B. Schneider[17], Y. J. Schnellbach[73], U. Schnoor[44], L. Schoeffel[137], A. Schoening[58b], B. D. Schoenrock[89], A. L. S. Schorlemmer[54], M. Schott[82], D. Schouten[160a], J. Schovancova[25], S. Schramm[159], M. Schreyer[175], C. Schroeder[82], N. Schuh[82], M. J. Schultens[21], H.-C. Schultz-Coulon[58a], H. Schulz[16], M. Schumacher[48], B. A. Schumm[138], Ph. Schune[137], A. Schwartzman[144], Ph. Schwegler[100], Ph. Schwemling[137], R. Schwienhorst[89], J. Schwindling[137], T. Schwindt[21], M. Schwoerer[5], F. G. Sciacca[17], E. Scifo[116], G. Sciolla[23], W. G. Scott[130], F. Scuri[123a,123b], F. Scutti[21], J. Searcy[88], G. Sedov[42], E. Sedykh[122], S. C. Seidel[104], A. Seiden[138], F. Seifert[127], J. M. Seixas[24a], G. Sekhniaidze[103a], S. J. Sekula[40], K. E. Selbach[46], D. M. Seliverstov[122,*], G. Sellers[73], N. Semprini-Cesari[20a,20b], C. Serfon[30], L. Serin[116], L. Serkin[54], T. Serre[84], R. Seuster[160a], H. Severini[112], F. Sforza[100], A. Sfyrla[30], E. Shabalina[54], M. Shamim[115], L. Y. Shan[33a], J. T. Shank[22], Q. T. Shao[87], M. Shapiro[15], P. B. Shatalov[96], K. Shaw[165a,165b], P. Sherwood[77], S. Shimizu[66], C. O. Shimmin[164], M. Shimojima[101], M. Shiyakova[64], A. Shmeleva[95], M. J. Shochet[31], D. Short[119], S. Shrestha[63], E. Shulga[97], M. A. Shupe[7], S. Shushkevich[42], P. Sicho[126], D. Sidorov[113], A. Sidoti[133a], F. Siegert[44], Dj. Sijacki[13a], O. Silbert[173], J. Silva[125a,125d], Y. Silver[154], D. Silverstein[144], S. B. Silverstein[147a], V. Simak[127], O. Simard[5], Lj. Simic[13a], S. Simion[116], E. Simioni[82], B. Simmons[77], R. Simoniello[90a,90b], M. Simonyan[36], P. Sinervo[159], N. B. Sinev[115], V. Sipica[142], G. Siragusa[175], A. Sircar[78], A. N. Sisakyan[64,*], S. Yu. Sivoklokov[98], J. Sjölin[147a,147b], T. B. Sjursen[14], H. P. Skottowe[57], K. Yu. Skovpen[108], P. Skubic[112], M. Slater[18], T. Slavicek[127], K. Sliwa[162], V. Smakhtin[173], B. H. Smart[46], L. Smestad[14], S. Yu. Smirnov[97], Y. Smirnov[97], L. N. Smirnova[98,ad], O. Smirnova[80], K. M. Smith[53], M. Smizanska[71], K. Smolek[127], A. A. Snesarev[95], G. Snidero[75], S. Snyder[25], R. Sobie[170,h], F. Socher[44], A. Soffer[154], D. A. Soh[152,s], C. A. Solans[30], M. Solar[127], J. Solc[127], E. Yu. Soldatov[97], U. Soldevila[168], E. Solfaroli Camillocci[133a,133b], A. A. Solodkov[129], O. V. Solovyanov[129], V. Solovyev[122], P. Sommer[48], H. Y. Song[33b], N. Soni[1], A. Sood[15], A. Sopczak[127], V. Sopko[127], B. Sopko[127], V. Sorin[12], M. Sosebee[8], R. Soualah[165a,165c], P. Soueid[94], A. M. Soukharev[108], D. South[42], S. Spagnolo[72a,72b], F. Spanò[76], W. R. Spearman[57], R. Spighi[20a], G. Spigo[30], M. Spousta[128], T. Spreitzer[159], B. Spurlock[8], R. D. St. Denis[53], S. Staerz[44], J. Stahlman[121], R. Stamen[58a], E. Stanecka[39], R. W. Stanek[6], C. Stanescu[135a], M. Stanescu-Bellu[42], M. M. Stanitzki[42], S. Stapnes[118], E. A. Starchenko[129], J. Stark[55], P. Staroba[126], P. Starovoitov[42], R. Staszewski[39], P. Stavina[145a,*], G. Steele[53], P. Steinberg[25], B. Stelzer[143], H. J. Stelzer[30], O. Stelzer-Chilton[160a], H. Stenzel[52], S. Stern[100], G. A. Stewart[53], J. A. Stillings[21], M. C. Stockton[86], M. Stoebe[86], G. Stoicea[26a], P. Stolte[54], S. Stonjek[100], A. R. Stradling[8], A. Straessner[44], M. E. Stramaglia[17], J. Strandberg[148], S. Strandberg[147a,147b], A. Strandlie[118], E. Strauss[144], M. Strauss[112], P. Strizenec[145b], R. Ströhmer[175], D. M. Strom[115], R. Stroynowski[40], S. A. Stucci[17], B. Stugu[14], N. A. Styles[42], D. Su[144], J. Su[124], HS. Subramania[3], R. Subramaniam[78], A. Succurro[12], Y. Sugaya[117], C. Suhr[107], M. Suk[127], V. V. Sulin[95], S. Sultansoy[4c], T. Sumida[67], X. Sun[33a], J. E. Sundermann[48], K. Suruliz[140], G. Susinno[37a,37b], M. R. Sutton[150], Y. Suzuki[65], M. Svatos[126], S. Swedish[169], M. Swiatlowski[144], I. Sykora[145a], T. Sykora[128], D. Ta[89], K. Tackmann[42], J. Taenzer[159], A. Taffard[164], R. Tafirout[160a], N. Taiblum[154], Y. Takahashi[102], H. Takai[25], R. Takashima[68], H. Takeda[66], T. Takeshita[141], Y. Takubo[65], M. Talby[84], A. A. Talyshev[108,p], J. Y. C. Tam[175], M. C. Tamsett[78,ae], K. G. Tan[87], J. Tanaka[156], R. Tanaka[116], S. Tanaka[132], S. Tanaka[65], A. J. Tanasijczuk[143], K. Tani[66], N. Tannoury[84], S. Tapprogge[82], S. Tarem[153], F. Tarrade[29], G. F. Tartarelli[90a], P. Tas[128], M. Tasevsky[126], T. Tashiro[67], E. Tassi[37a,37b], A. Tavares Delgado[125a,125b], Y. Tayalati[136d], F. E. Taylor[93], G. N. Taylor[87], W. Taylor[160b], F. A. Teischinger[30], M. Teixeira Dias Castanheira[75], P. Teixeira-Dias[76], K. K. Temming[48], H. Ten Kate[30], P. K. Teng[152], S. Terada[65], K. Terashi[156], J. Terron[81], S. Terzo[100], M. Testa[47], R. J. Teuscher[159,h], J. Therhaag[21], T. Theveneaux-Pelzer[34], S. Thoma[48], J. P. Thomas[18], J. Thomas-Wilsker[76], E. N. Thompson[35], P. D. Thompson[18], P. D. Thompson[159], A. S. Thompson[53], L. A. Thomsen[36], E. Thomson[121], M. Thomson[28], W. M. Thong[87], R. P. Thun[88,*], F. Tian[35], M. J. Tibbetts[15], V. O. Tikhomirov[95,af], Yu. A. Tikhonov[108,p], S. Timoshenko[97], E. Tiouchichine[84], P. Tipton[177], S. Tisserant[84], T. Todorov[5], S. Todorova-Nova[128], B. Toggerson[7], J. Tojo[69], S. Tokár[145a], K. Tokushuku[65], K. Tollefson[89], L. Tomlinson[83], M. Tomoto[102], L. Tompkins[31], K. Toms[104], N. D. Topilin[64], E. Torrence[115], H. Torres[143], E. Torró Pastor[168], J. Toth[84,aa], F. Touchard[84], D. R. Tovey[140], H. L. Tran[116], T. Trefzger[175], L. Tremblet[30], A. Tricoli[30], I. M. Trigger[160a], S. Trincaz-Duvoid[79], M. F. Tripiana[70], N. Triplett[25], W. Trischuk[159], B. Trocmé[55], C. Troncon[90a], M. Trottier-McDonald[143], M. Trovatelli[135a,135b], P. True[89], M. Trzebinski[39], A. Trzupek[39], C. Tsarouchas[30], J. C-L. Tseng[119], P. V. Tsiareshka[91], D. Tsionou[137], G. Tsipolitis[10], N. Tsirintanis[9], S. Tsiskaridze[12], V. Tsiskaridze[48], E. G. Tskhadadze[51a], I. I. Tsukerman[96], V. Tsulaia[15], S. Tsuno[65], D. Tsybychev[149], A. Tudorache[26a], V. Tudorache[26a], A. N. Tuna[121], S. A. Tupputi[20a,20b], S. Turchikhin[98,ad], D. Turecek[127], I. Turk Cakir[4d], R. Turra[90a,90b], P. M. Tuts[35], A. Tykhonov[74], M. Tylmad[147a,147b], M. Tyndel[130], K. Uchida[21], I. Ueda[156], R. Ueno[29], M. Ughetto[84], M. Ugland[14], M. Uhlenbrock[21], F. Ukegawa[161], G. Unal[30], A. Undrus[25], G. Unel[164], F. C. Ungaro[48], Y. Unno[65], D. Urbaniec[35], P. Urquijo[21], G. Usai[8], A. Usanova[61], L. Vacavant[84], V. Vacek[127], B. Vachon[86], N. Valencic[106], S. Valentinetti[20a,20b], A. Valero[168], L. Valery[34], S. Valkar[128], E. Valladolid Gallego[168], S. Vallecorsa[49], J. A. Valls Ferrer[168], P. C. Van Der Deijl[106], R. van der Geer[106], H. van der Graaf[106], R. Van Der Leeuw[106], D. van der Ster[30], N. van Eldik[30], P. van Gemmeren[6], J. Van Nieuwkoop[143], I. van Vulpen[106], M. C. van Woerden[30], M. Vanadia[133a,133b], W. Vandelli[30], R. Vanguri[121], A. Vaniachine[6], P. Vankov[42], F. Vannucci[79], G. Vardanyan[178], R. Vari[133a], E. W. Varnes[7], T. Varol[85], D. Varouchas[79], A.

Vartapetian[8], K. E. Varvell[151], F. Vazeille[34], T. Vazquez Schroeder[54], J. Veatch[7], F. Veloso[125a,125c], S. Veneziano[133a], A. Ventura[72a,72b], D. Ventura[85], M. Venturi[48], N. Venturi[159], A. Venturini[23], V. Vercesi[120a], M. Verducci[139], W. Verkerke[106], J. C. Vermeulen[106], A. Vest[44], M. C. Vetterli[143,d], O. Viazlo[80], I. Vichou[166], T. Vickey[146c,ag], O. E. Vickey Boeriu[146c], G. H. A. Viehhauser[119], S. Viel[169], R. Vigne[30], M. Villa[20a,20b], M. Villaplana Perez[168], E. Vilucchi[47], M. G. Vincter[29], V. B. Vinogradov[64], J. Virzi[15], I. Vivarelli[150], F. Vives Vaque[3], S. Vlachos[10], D. Vladoiu[99], M. Vlasak[127], A. Vogel[21], P. Vokac[127], G. Volpi[123a,123b], M. Volpi[87], H. von der Schmitt[100], H. von Radziewski[48], E. von Toerne[21], V. Vorobel[128], K. Vorobev[97], M. Vos[168], R. Voss[30], J. H. Vossebeld[73], N. Vranjes[137], M. Vranjes Milosavljevic[106], V. Vrba[126], M. Vreeswijk[106], T. Vu Anh[48], R. Vuillermet[30], I. Vukotic[31], Z. Vykydal[127], W. Wagner[176], P. Wagner[21], S. Wahrmund[44], J. Wakabayashi[102], J. Walder[71], R. Walker[99], W. Walkowiak[142], R. Wall[177], P. Waller[73], B. Walsh[177], C. Wang[152,ah], C. Wang[45], F. Wang[174], H. Wang[15], H. Wang[40], J. Wang[42], J. Wang[33a], K. Wang[86], R. Wang[104], S. M. Wang[152], T. Wang[21], X. Wang[177], C. Wanotayaroj[115], A. Warburton[86], C. P. Ward[28], D. R. Wardrope[77], M. Warsinsky[48], A. Washbrook[46], C. Wasicki[42], I. Watanabe[66], P. M. Watkins[18], A. T. Watson[18], I. J. Watson[151], M. F. Watson[18], G. Watts[139], S. Watts[83], B. M. Waugh[77], S. Webb[83], M. S. Weber[17], S. W. Weber[175], J. S. Webster[31], A. R. Weidberg[119], P. Weigell[100], B. Weinert[60], J. Weingarten[54], C. Weiser[48], H. Weits[106], P. S. Wells[30], T. Wenaus[25], D. Wendland[16], Z. Weng[152,s], T. Wengler[30], S. Wenig[30], N. Wermes[21], M. Werner[48], P. Werner[30], M. Wessels[58a], J. Wetter[162], K. Whalen[29], A. White[8], M. J. White[1], R. White[32b], S. White[123a,123b], D. Whiteson[164], D. Wicke[176], F. J. Wickens[130], W. Wiedenmann[174], M. Wielers[130], P. Wienemann[21], C. Wiglesworth[36], L. A. M. Wiik-Fuchs[21], P. A. Wijeratne[77], A. Wildauer[100], M. A. Wildt[42,ai], H. G. Wilkens[30], J. Z. Will[99], H. H. Williams[121], S. Williams[28], C. Willis[89], S. Willocq[85], J. A. Wilson[18], A. Wilson[88], I. Wingerter-Seez[5], F. Winklmeier[115], M. Wittgen[144], T. Wittig[43], J. Wittkowski[99], S. J. Wollstadt[82], M. W. Wolter[39], H. Wolters[125a,125c], B. K. Wosiek[39], J. Wotschack[30], M. J. Woudstra[83], K. W. Wozniak[39], M. Wright[53], M. Wu[55], S. L. Wu[174], X. Wu[49], Y. Wu[88], E. Wulf[35], T. R. Wyatt[83], B. M. Wynne[46], S. Xella[36], M. Xiao[137], D. Xu[33a], L. Xu[33b,aj], B. Yabsley[151], S. Yacoob[146b,ak], M. Yamada[65], H. Yamaguchi[156], Y. Yamaguchi[156], A. Yamamoto[65], K. Yamamoto[63], S. Yamamoto[156], T. Yamamura[156], T. Yamanaka[156], K. Yamauchi[102], Y. Yamazaki[66], Z. Yan[22], H. Yang[33e], H. Yang[174], U. K. Yang[83], Y. Yang[110], S. Yanush[92], L. Yao[33a], W-M. Yao[15], Y. Yasu[65], E. Yatsenko[42], K. H. Yau Wong[21], J. Ye[40], S. Ye[25], A. L. Yen[57], E. Yildirim[42], M. Yilmaz[4b], R. Yoosoofmiya[124], K. Yorita[172], R. Yoshida[6], K. Yoshihara[156], C. Young[144], C. J. S. Young[30], S. Youssef[22], D. R. Yu[15], J. Yu[8], J. M. Yu[88], J. Yu[113], L. Yuan[66], A. Yurkewicz[107], B. Zabinski[39], R. Zaidan[62], A. M. Zaitsev[129,x], A. Zaman[149], S. Zambito[23], L. Zanello[133a,133b], D. Zanzi[100], A. Zaytsev[25], C. Zeitnitz[176], M. Zeman[127], A. Zemla[38a], K. Zengel[23], O. Zenin[129], T. Ženiš[145a], D. Zerwas[116], G. Zevi della Porta[57], D. Zhang[88], F. Zhang[174], H. Zhang[89], J. Zhang[6], L. Zhang[152], X. Zhang[33d], Z. Zhang[116], Z. Zhao[33b], A. Zhemchugov[64], J. Zhong[119], B. Zhou[88], L. Zhou[35], N. Zhou[164], C. G. Zhu[33d], H. Zhu[33a], J. Zhu[88], Y. Zhu[33b], X. Zhuang[33a], A. Zibell[175], D. Zieminska[60], N. I. Zimine[64], C. Zimmermann[82], R. Zimmermann[21], S. Zimmermann[21], S. Zimmermann[48], Z. Zinonos[54], M. Ziolkowski[142], G. Zobernig[174], A. Zoccoli[20a,20b], M. zur Nedden[16], G. Zurzolo[103a,103b], V. Zutshi[107], L. Zwalinski[30]

1 Department of Physics, University of Adelaide, Adelaide, Australia

2 Physics Department, SUNY Albany, Albany, NY, USA

3 Department of Physics, University of Alberta, Edmonton, AB, Canada

4 (a) Department of Physics, Ankara University, Ankara, Turkey; (b) Department of Physics, Gazi University, Ankara, Turkey; (c) Division of Physics, TOBB University of Economics and Technology, Ankara, Turkey; (d) Turkish Atomic Energy Authority, Ankara, Turkey

5 LAPP, CNRS/IN2P3 and Université de Savoie, Annecy-le-Vieux, France

6 High Energy Physics Division, Argonne National Laboratory, Argonne, IL, USA

7 Department of Physics, University of Arizona, Tucson, AZ, USA

8 Department of Physics, The University of Texas at Arlington, Arlington, TX, USA

9 Physics Department, University of Athens, Athens, Greece

10 Physics Department, National Technical University of Athens, Zografou, Greece

11 Institute of Physics, Azerbaijan Academy of Sciences, Baku, Azerbaijan

12 Institut de Física d'Altes Energies and Departament de Física de la Universitat Autònoma de Barcelona, Barcelona, Spain

13 (a) Institute of Physics, University of Belgrade, Belgrade, Serbia; (b) Vinca Institute of Nuclear Sciences, University of Belgrade, Belgrade, Serbia

14 Department for Physics and Technology, University of Bergen, Bergen, Norway

15 Physics Division, Lawrence Berkeley National Laboratory and University of California, Berkeley, CA, USA

16 Department of Physics, Humboldt University, Berlin, Germany

17 Albert Einstein Center for Fundamental Physics and Laboratory for High Energy Physics, University of Bern, Bern, Switzerland

18 School of Physics and Astronomy, University of Birmingham, Birmingham, UK

19 (a) Department of Physics, Bogazici University, Istanbul, Turkey; (b) Department of Physics, Dogus University, Istanbul, Turkey; (c) Department of Physics Engineering, Gaziantep University, Gaziantep, Turkey

20 (a) INFN Sezione di Bologna, Bologna, Italy; (b) Dipartimento di Fisica e Astronomia, Università di Bologna, Bologna, Italy

21 Physikalisches Institut, University of Bonn, Bonn, Germany

22 Department of Physics, Boston University, Boston, MA, USA

23 Department of Physics, Brandeis University, Waltham, MA, USA

24 (a) Universidade Federal do Rio De Janeiro COPPE/EE/IF, Rio de Janeiro, Brazil; (b) Federal University of Juiz de Fora (UFJF), Juiz de Fora, Brazil; (c) Federal University of Sao Joao del Rei (UFSJ), Sao Joao del Rei, Brazil; (d) Instituto de Fisica, Universidade de Sao Paulo, Sao Paulo, Brazil

25 Physics Department, Brookhaven National Laboratory, Upton, NY, USA

26 (a) National Institute of Physics and Nuclear Engineering, Bucharest, Romania; (b) Physics Department, National Institute for Research and Development of Isotopic and Molecular Technologies, Cluj Napoca, Romania; (c) University Politehnica Bucharest, Bucharest, Romania; (d) West University in Timisoara, Timisoara, Romania

27 Departamento de Física, Universidad de Buenos Aires, Buenos Aires, Argentina

28 Cavendish Laboratory, University of Cambridge, Cambridge, UK

29 Department of Physics, Carleton University, Ottawa, ON, Canada

30 CERN, Geneva, Switzerland

31 Enrico Fermi Institute, University of Chicago, Chicago, IL, USA

32 (a) Departamento de Física, Pontificia Universidad Católica de Chile, Santiago, Chile; (b) Departamento de Física, Universidad Técnica Federico Santa María, Valparaiso, Chile

33 (a) Institute of High Energy Physics, Chinese Academy of Sciences, Beijing, China; (b) Department of Modern Physics, University of Science and Technology of China, Hefei, Anhui, China; (c) Department of Physics, Nanjing University, Nanjing, Jiangsu, China; (d) School of Physics, Shandong University, Jinan, Shandong, China; (e) Physics Department,, Shanghai Jiao Tong University, Shanghai, China

34 Laboratoire de Physique Corpusculaire, Clermont Université and Université Blaise Pascal and CNRS/IN2P3, Clermont-Ferrand, France

35 Nevis Laboratory, Columbia University, Irvington, NY, USA

36 Niels Bohr Institute, University of Copenhagen, Copenhagen, Denmark

37 (a) INFN Gruppo Collegato di Cosenza, Laboratori Nazionali di Frascati, Frascati, Italy; (b) Dipartimento di Fisica, Università della Calabria, Rende, Italy

38 (a) Faculty of Physics and Applied Computer Science, AGH University of Science and Technology, Kraków, Poland; (b) Marian Smoluchowski Institute of Physics, Jagiellonian University, Kraków, Poland

39 The Henryk Niewodniczanski Institute of Nuclear Physics, Polish Academy of Sciences, Kraków, Poland

40 Physics Department, Southern Methodist University, Dallas, TX, USA

41 Physics Department, University of Texas at Dallas, Richardson, TX, USA

42 DESY, Hamburg and Zeuthen, Germany

43 Institut für Experimentelle Physik IV, Technische Universität Dortmund, Dortmund, Germany

44 Institut für Kern- und Teilchenphysik, Technische Universität Dresden, Dresden, Germany

45 Department of Physics, Duke University, Durham, NC, USA

46 SUPA-School of Physics and Astronomy, University of Edinburgh, Edinburgh, UK

47 INFN Laboratori Nazionali di Frascati, Frascati, Italy

48 Fakultät für Mathematik und Physik, Albert-Ludwigs-Universität, Freiburg, Germany

49 Section de Physique, Université de Genève, Geneva, Switzerland

50 (a) INFN Sezione di Genova, Genoa, Italy; (b) Dipartimento di Fisica, Università di Genova, Genoa, Italy

51 (a) E. Andronikashvili Institute of Physics, Iv. Javakhishvili Tbilisi State University, Tbilisi, Georgia; (b) High Energy Physics Institute, Tbilisi State University, Tbilisi, Georgia

52 II Physikalisches Institut, Justus-Liebig-Universität Giessen, Giessen, Germany

53 SUPA-School of Physics and Astronomy, University of Glasgow, Glasgow, UK

54 II Physikalisches Institut, Georg-August-Universität, Göttingen, Germany

55 Laboratoire de Physique Subatomique et de Cosmologie, Université Grenoble-Alpes, CNRS/IN2P3, Grenoble, France

56 Department of Physics, Hampton University, Hampton, VA, USA

[57] Laboratory for Particle Physics and Cosmology, Harvard University, Cambridge, MA, USA

[58] (a) Kirchhoff-Institut für Physik, Ruprecht-Karls-Universität Heidelberg, Heidelberg, Germany; (b) Physikalisches Institut, Ruprecht-Karls-Universität Heidelberg, Heidelberg, Germany; (c) ZITI Institut für technische Informatik, Ruprecht-Karls-Universität Heidelberg, Mannheim, Germany

[59] Faculty of Applied Information Science, Hiroshima Institute of Technology, Hiroshima, Japan

[60] Department of Physics, Indiana University, Bloomington, IN, USA

[61] Institut für Astro- und Teilchenphysik, Leopold-Franzens-Universität, Innsbruck, Austria

[62] University of Iowa, Iowa City, IA, USA

[63] Department of Physics and Astronomy, Iowa State University, Ames, IA, USA

[64] Joint Institute for Nuclear Research, JINR Dubna, Dubna, Russia

[65] KEK, High Energy Accelerator Research Organization, Tsukuba, Japan

[66] Graduate School of Science, Kobe University, Kobe, Japan

[67] Faculty of Science, Kyoto University, Kyoto, Japan

[68] Kyoto University of Education, Kyoto, Japan

[69] Department of Physics, Kyushu University, Fukuoka, Japan

[70] Instituto de Física La Plata, Universidad Nacional de La Plata and CONICET, La Plata, Argentina

[71] Physics Department, Lancaster University, Lancaster, UK

[72] (a) INFN Sezione di Lecce, Lecce, Italy; (b) Dipartimento di Matematica e Fisica, Università del Salento, Lecce, Italy

[73] Oliver Lodge Laboratory, University of Liverpool, Liverpool, UK

[74] Department of Physics, Jožef Stefan Institute and University of Ljubljana, Ljubljana, Slovenia

[75] School of Physics and Astronomy, Queen Mary University of London, London, UK

[76] Department of Physics, Royal Holloway University of London, Surrey, UK

[77] Department of Physics and Astronomy, University College London, London, UK

[78] Louisiana Tech University, Ruston, LA, USA

[79] Laboratoire de Physique Nucléaire et de Hautes Energies, UPMC and Université Paris-Diderot and CNRS/IN2P3, Paris, France

[80] Fysiska institutionen, Lunds universitet, Lund, Sweden

[81] Departamento de Fisica Teorica C-15, Universidad Autonoma de Madrid, Madrid, Spain

[82] Institut für Physik, Universität Mainz, Mainz, Germany

[83] School of Physics and Astronomy, University of Manchester, Manchester, UK

[84] CPPM, Aix-Marseille Université and CNRS/IN2P3, Marseille, France

[85] Department of Physics, University of Massachusetts, Amherst, MA, USA

[86] Department of Physics, McGill University, Montreal, QC, Canada

[87] School of Physics, University of Melbourne, Parkville, VIC, Australia

[88] Department of Physics, The University of Michigan, Ann Arbor, MI, USA

[89] Department of Physics and Astronomy, Michigan State University, East Lansing, MI, USA

[90] (a) INFN Sezione di Milano, Milan, Italy; (b) Dipartimento di Fisica, Università di Milano, Milan, Italy

[91] B.I. Stepanov Institute of Physics, National Academy of Sciences of Belarus, Minsk, Republic of Belarus

[92] National Scientific and Educational Centre for Particle and High Energy Physics, Minsk, Republic of Belarus

[93] Department of Physics, Massachusetts Institute of Technology, Cambridge, MA, USA

[94] Group of Particle Physics, University of Montreal, Montreal, QC, Canada

[95] P.N. Lebedev Institute of Physics, Academy of Sciences, Moscow, Russia

[96] Institute for Theoretical and Experimental Physics (ITEP), Moscow, Russia

[97] Moscow Engineering and Physics Institute (MEPhI), Moscow, Russia

[98] D.V.Skobeltsyn Institute of Nuclear Physics, M.V.Lomonosov Moscow State University, Moscow, Russia

[99] Fakultät für Physik, Ludwig-Maximilians-Universität München, Munich, Germany

[100] Max-Planck-Institut für Physik (Werner-Heisenberg-Institut), Munich, Germany

[101] Nagasaki Institute of Applied Science, Nagasaki, Japan

[102] Graduate School of Science and Kobayashi-Maskawa Institute, Nagoya University, Nagoya, Japan

[103] (a) INFN Sezione di Napoli, Naples, Italy; (b) Dipartimento di Fisica, Università di Napoli, Naples, Italy

[104] Department of Physics and Astronomy, University of New Mexico, Albuquerque, NM, USA

[105] Institute for Mathematics, Astrophysics and Particle Physics, Radboud University Nijmegen/Nikhef, Nijmegen, Netherlands

[106] Nikhef National Institute for Subatomic Physics and University of Amsterdam, Amsterdam, The Netherlands

[107] Department of Physics, Northern Illinois University, DeKalb, IL, USA

[108] Budker Institute of Nuclear Physics, SB RAS, Novosibirsk, Russia

[109] Department of Physics, New York University, New York, NY, USA

[110] Ohio State University, Columbus, OH, USA

[111] Faculty of Science, Okayama University, Okayama, Japan

[112] Homer L. Dodge Department of Physics and Astronomy, University of Oklahoma, Norman, OK, USA

[113] Department of Physics, Oklahoma State University, Stillwater, OK, USA

[114] Palacký University, RCPTM, Olomouc, Czech Republic

[115] Center for High Energy Physics, University of Oregon, Eugene, OR, USA

[116] LAL, Université Paris-Sud and CNRS/IN2P3, Orsay, France

[117] Graduate School of Science, Osaka University, Osaka, Japan

[118] Department of Physics, University of Oslo, Oslo, Norway

[119] Department of Physics, Oxford University, Oxford, UK

[120] (a) INFN Sezione di Pavia, Pavia, Italy; (b) Dipartimento di Fisica, Università di Pavia, Pavia, Italy

[121] Department of Physics, University of Pennsylvania, Philadelphia, PA, USA

[122] Petersburg Nuclear Physics Institute, Gatchina, Russia

[123] (a) INFN Sezione di Pisa, Pisa, Italy; (b) Dipartimento di Fisica E. Fermi, Università di Pisa, Pisa, Italy

[124] Department of Physics and Astronomy, University of Pittsburgh, Pittsburgh, PA, USA

[125] (a) Laboratorio de Instrumentacao e Fisica Experimental de Particulas-LIP, Lisbon, Portugal; (b) Faculdade de Ciências, Universidade de Lisboa, Lisboa, Portugal; (c) Department of Physics, University of Coimbra, Coimbra, Portugal; (d) Centro de Física Nuclear da Universidade de Lisboa, Lisbon, Portugal; (e) Departamento de Fisica, Universidade do Minho, Braga, Portugal; (f) Departamento de Fisica Teorica y del Cosmos and CAFPE, Universidad de Granada, Granada, Spain; (g) Dep Fisica and CEFITEC of Faculdade de Ciencias e Tecnologia, Universidade Nova de Lisboa, Caparica, Portugal

[126] Institute of Physics, Academy of Sciences of the Czech Republic, Prague, Czech Republic

[127] Czech Technical University in Prague, Prague, Czech Republic

[128] Faculty of Mathematics and Physics, Charles University in Prague, Prague, Czech Republic

[129] State Research Center Institute for High Energy Physics, Protvino, Russia

[130] Particle Physics Department, Rutherford Appleton Laboratory, Didcot, UK

[131] Physics Department, University of Regina, Regina, SK, Canada

[132] Ritsumeikan University, Kusatsu, Shiga, Japan

[133] (a) INFN Sezione di Roma, Rome, Italy; (b) Dipartimento di Fisica, Sapienza Università di Roma, Rome, Italy

[134] (a) INFN Sezione di Roma Tor Vergata, Rome, Italy; (b) Dipartimento di Fisica, Università di Roma Tor Vergata, Rome, Italy

[135] (a) INFN Sezione di Roma Tre, Rome, Italy; (b) Dipartimento di Matematica e Fisica, Università Roma Tre, Rome, Italy

[136] (a) Faculté des Sciences Ain Chock, Réseau Universitaire de Physique des Hautes Energies-Université Hassan II, Casablanca, Morocco; (b) Centre National de l'Energie des Sciences Techniques Nucleaires, Rabat, Morocco; (c) Faculté des Sciences Semlalia, Université Cadi Ayyad, LPHEA-Marrakech, Marrakech, Morocco; (d) Faculté des Sciences, Université Mohamed Premier and LPTPM, Oujda, Morocco; (e) Faculté des Sciences, Université Mohammed V-Agdal, Rabat, Morocco

[137] DSM/IRFU (Institut de Recherches sur les Lois Fondamentales de l'Univers), CEA Saclay (Commissariat à l'Energie Atomique et aux Energies Alternatives), Gif-sur-Yvette, France

[138] Santa Cruz Institute for Particle Physics, University of California Santa Cruz, Santa Cruz, CA, USA

[139] Department of Physics, University of Washington, Seattle, WA, USA

[140] Department of Physics and Astronomy, University of Sheffield, Sheffield, UK

[141] Department of Physics, Shinshu University, Nagano, Japan

[142] Fachbereich Physik, Universität Siegen, Siegen, Germany

[143] Department of Physics, Simon Fraser University, Burnaby, BC, Canada

[144] SLAC National Accelerator Laboratory, Stanford, CA, USA

[145] (a) Faculty of Mathematics, Physics and Informatics, Comenius University, Bratislava, Slovak Republic; (b) Department of Subnuclear Physics, Institute of Experimental Physics of the Slovak Academy of Sciences, Kosice, Slovak Republic

146 (a) Department of Physics, University of Cape Town, Cape Town, South Africa; (b) Department of Physics, University of Johannesburg, Johannesburg, South Africa; (c) School of Physics, University of the Witwatersrand, Johannesburg, South Africa

147 (a) Department of Physics, Stockholm University, Stockholm, Sweden; (b) The Oskar Klein Centre, Stockholm, Sweden

148 Physics Department, Royal Institute of Technology, Stockholm, Sweden

149 Departments of Physics and Astronomy and Chemistry, Stony Brook University, Stony Brook, NY, USA

150 Department of Physics and Astronomy, University of Sussex, Brighton, UK

151 School of Physics, University of Sydney, Sydney, Australia

152 Institute of Physics, Academia Sinica, Taipei, Taiwan

153 Department of Physics, Technion: Israel Institute of Technology, Haifa, Israel

154 Raymond and Beverly Sackler School of Physics and Astronomy, Tel Aviv University, Tel Aviv, Israel

155 Department of Physics, Aristotle University of Thessaloniki, Thessaloniki, Greece

156 International Center for Elementary Particle Physics and Department of Physics, The University of Tokyo, Tokyo, Japan

157 Graduate School of Science and Technology, Tokyo Metropolitan University, Tokyo, Japan

158 Department of Physics, Tokyo Institute of Technology, Tokyo, Japan

159 Department of Physics, University of Toronto, Toronto, ON, Canada

160 (a) TRIUMF, Vancouver, BC, Canada; (b) Department of Physics and Astronomy, York University, Toronto, ON, Canada

161 Faculty of Pure and Applied Sciences, University of Tsukuba, Tsukuba, Japan

162 Department of Physics and Astronomy, Tufts University, Medford, MA, USA

163 Centro de Investigaciones, Universidad Antonio Narino, Bogota, Colombia

164 Department of Physics and Astronomy, University of California Irvine, Irvine, CA, USA

165 (a) INFN Gruppo Collegato di Udine, Sezione di Trieste, Udine, Italy; (b) ICTP, Trieste, Italy; (c) Dipartimento di Chimica, Fisica e Ambiente, Università di Udine, Udine, Italy

166 Department of Physics, University of Illinois, Urbana, IL, USA

167 Department of Physics and Astronomy, University of Uppsala, Uppsala, Sweden

168 Instituto de Física Corpuscular (IFIC) and Departamento de Física Atómica, Molecular y Nuclear and Departamento de Ingeniería Electrónica and Instituto de Microelectrónica de Barcelona (IMB-CNM), University of Valencia and CSIC, Valencia, Spain

169 Department of Physics, University of British Columbia, Vancouver, BC, Canada

170 Department of Physics and Astronomy, University of Victoria, Victoria, BC, Canada

171 Department of Physics, University of Warwick, Coventry, UK

172 Waseda University, Tokyo, Japan

173 Department of Particle Physics, The Weizmann Institute of Science, Rehovot, Israel

174 Department of Physics, University of Wisconsin, Madison, WI, USA

175 Fakultät für Physik und Astronomie, Julius-Maximilians-Universität, Würzburg, Germany

176 Fachbereich C Physik, Bergische Universität Wuppertal, Wuppertal, Germany

177 Department of Physics, Yale University, New Haven, CT, USA

178 Yerevan Physics Institute, Yerevan, Armenia

179 Centre de Calcul de l'Institut National de Physique Nucléaire et de Physique des Particules (IN2P3), Villeurbanne, France

a Also at Department of Physics, King's College London, London, UK

b Also at Institute of Physics, Azerbaijan Academy of Sciences, Baku, Azerbaijan

c Also at Particle Physics Department, Rutherford Appleton Laboratory, Didcot, UK

d Also at TRIUMF, Vancouver, BC, Canada

e Also at Department of Physics, California State University, Fresno, CA, USA

f Also at CPPM, Aix-Marseille Université and CNRS/IN2P3, Marseille, France

g Also at Università di Napoli Parthenope, Naples, Italy

h Also at Institute of Particle Physics (IPP), Canada

i Also at Department of Physics, St. Petersburg State Polytechnical University, St. Petersburg, Russia

j Also at Department of Financial and Management Engineering, University of the Aegean, Chios, Greece

k Also at Louisiana Tech University, Ruston, LA, USA

l Also at Institucio Catalana de Recerca i Estudis Avancats, ICREA, Barcelona, Spain

ᵐ Also at CERN, Geneva, Switzerland

ⁿ Also at Ochadai Academic Production, Ochanomizu University, Tokyo, Japan

ᵒ Also at Manhattan College, New York, NY, USA

ᵖ Also at Novosibirsk State University, Novosibirsk, Russia

�q Also at Institute of Physics, Academia Sinica, Taipei, Taiwan

ʳ Also at LAL, Université Paris-Sud and CNRS/IN2P3, Orsay, France

ˢ Also at School of Physics and Engineering, Sun Yat-sen University, Guangzhou, China

ᵗ Also at Academia Sinica Grid Computing, Institute of Physics, Academia Sinica, Taipei, Taiwan

ᵘ Also at Laboratoire de Physique Nucléaire et de Hautes Energies, UPMC and Université Paris-Diderot and CNRS/IN2P3, Paris, France

ᵛ Also at School of Physical Sciences, National Institute of Science Education and Research, Bhubaneswar, India

ʷ Also at Dipartimento di Fisica, Sapienza Università di Roma, Rome, Italy

ˣ Also at Moscow Institute of Physics and Technology State University, Dolgoprudny, Russia

ʸ Also at Section de Physique, Université de Genève, Geneva, Switzerland

ᶻ Also at Department of Physics, The University of Texas at Austin, Austin, TX, USA

ᵃᵃ Also at Institute for Particle and Nuclear Physics, Wigner Research Centre for Physics, Budapest, Hungary

ᵃᵇ Also at International School for Advanced Studies (SISSA), Trieste, Italy

ᵃᶜ Also at Department of Physics and Astronomy, University of South Carolina, Columbia, SC, USA

ᵃᵈ Also at Faculty of Physics, M.V.Lomonosov Moscow State University, Moscow, Russia

ᵃᵉ Also at Physics Department, Brookhaven National Laboratory, Upton, NY, USA

ᵃᶠ Also at Moscow Engineering and Physics Institute (MEPhI), Moscow, Russia

ᵃᵍ Also at Department of Physics, Oxford University, Oxford, UK

ᵃʰ Also at Department of Physics, Nanjing University, Jiangsu, China

ᵃⁱ Also at Institut für Experimentalphysik, Universität Hamburg, Hamburg, Germany

ᵃʲ Also at Department of Physics, The University of Michigan, Ann Arbor, MI, USA

ᵃᵏ Also at Discipline of Physics, University of KwaZulu-Natal, Durban, South Africa

* Deceased